

Pinpoint-fluorinated Polycyclic Aromatic Hydrocarbons (F-PAHs): Syntheses of Difluorinated Subfamily and Their Properties

Kohei Fuchibe^a, Kento Shigeno^a, Nan Zhao^a, Hiromichi Aihara^a, Rikuo Akisaka^a, Toshiyuki Morikawa^a, Takeshi Fujita^a, Kie Yamakawa^b, Toshihiro Shimada^b, and Junji Ichikawa^{a*}

^a Division of Chemistry, Faculty of Pure and Applied Sciences, University of Tsukuba, Tsukuba, Ibaraki 305-8571, Japan

^b Division of Applied Chemistry, Graduate School of Engineering, Hokkaido University, Sapporo, Hokkaido 060-8628, Japan

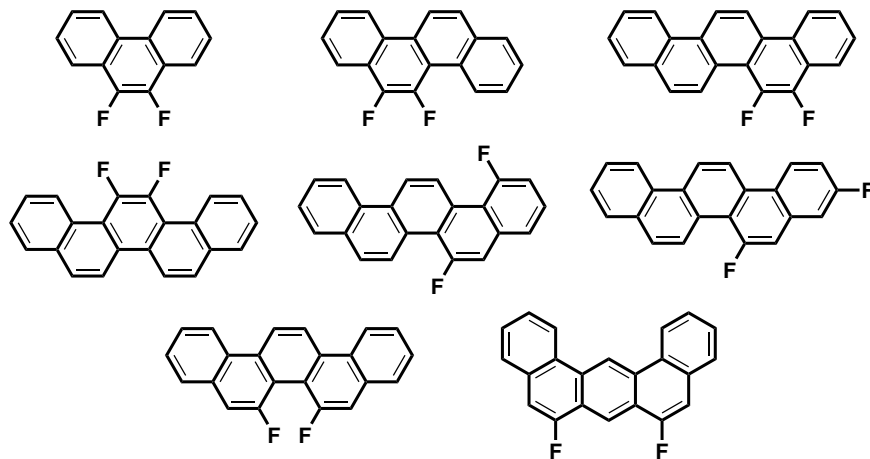
KEYWORDS:

Cyclization, Fluoroalkenes, Fluoroallenes, Polycyclic aromatic hydrocarbons, Solubility, Semiconductors

Dedicated to Professor Antonio Togni with recognition on the occasion of his being awarded the 2017 ACS Award for Creative Work in Fluorine Chemistry.

ABSTRACT: Difluorinated polycyclic aromatic hydrocarbons (PAHs) containing three to five benzene rings were systematically synthesized by the Pd(II)-catalyzed Friedel–Crafts-type cyclization of 1,1,2-trifluoro- and 1,1-difluoro-1-alkenes and the In(III)-catalyzed tandem cyclization of bis(1,1-difluoroallene)s. Using an array of the difluorinated PAHs that were obtained and previously reported monofluorinated PAHs, the physical properties of the pinpoint-fluorinated PAHs were investigated. (i) The ¹⁹F NMR signals of the bay-region fluorine atoms were shifted downfield by ca. 8–14 ppm for *vic*-difluorinated PAHs and ca. 11–19 ppm for non-*vic*-difluorinated and monofluorinated PAHs. (ii) The introduction of fluorine into PAH molecules increased their solubilities in organic solvents, which was best exemplified by the high solubilities of 6,7-difluoropicene (5.4 wt%) and 6-fluoropicene (5.3 wt%) in THF. (iii) The HOMO–LUMO energy gaps of the pinpoint-fluorinated PAHs were smaller than that

of the corresponding fluorine-free PAH (i.e., picene) by 0.02–0.26 eV, and the HOMO and LUMO energy levels were lowered by 0.10–0.22 eV and 0.12–0.41 eV, respectively.



1. Introduction

Polycyclic aromatic hydrocarbons (PAHs) are compounds that comprise ortho- and/or peri-fused benzene rings in various configurations [1]. Acenes and phenacenes are representatives of this class of molecules with a linear and zigzag configuration, respectively. Importance of these PAHs as organic semiconducting materials is increasing significantly in the field of materials science [2]. Therefore, the development of methods for the synthesis of PAHs is becoming an important issue.

Regioselectively mono- or difluorinated (pinpoint-fluorinated) PAHs (F-PAHs, Figure 1) are a promising class of organic semiconducting materials because of the unique properties of the fluorine substituent(s) (Figure 2) [3]: (a) The high electronegativity of fluorine leads to an increase in the resistance of the fluorinated PAHs to aerial oxidation by lowering the energy levels of their HOMO. (b) The repulsive interaction between the lone pairs in the fluorine 2p orbitals and the adjacent π -electrons in the carbon 2p orbitals perturbs the electron distribution in the extended π -system [4]. The induced polarization renders PAHs highly soluble in polar solvents, leading to printable organic electronic devices [5]. (c) From the viewpoint of steric bulk, the low steric demand of fluorine, the introduction of which into PAHs causes no significant change in their molecular shape, would have little effect on their π - π stacking in the solid state. Thus, the electronic and steric effects of attaching single or double

fluorine substituent(s) to PAH skeletons can endow them with advantageous semiconducting properties, as exemplified by fluorinated picones, which are soluble in THF and exhibit p-type semiconducting behavior [6,7].

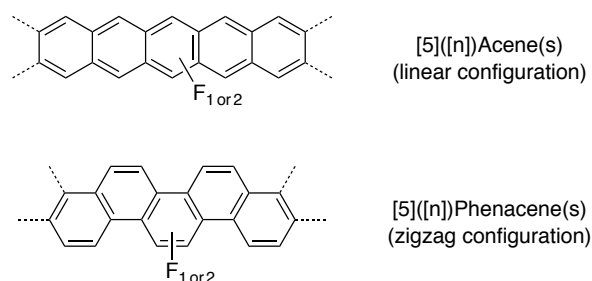


Figure 1. Structures of pinpoint-fluorinated acenes and phenacenes (n refers to the number of benzene rings).

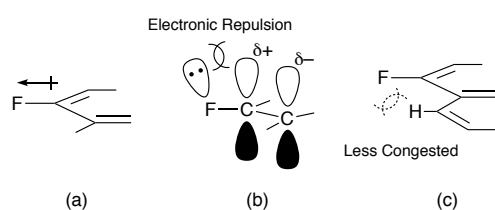
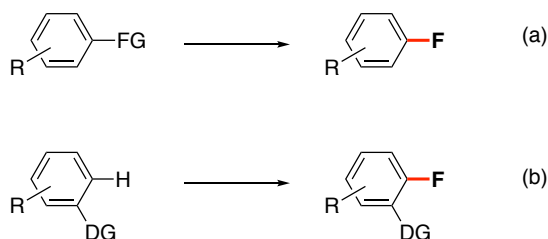


Figure 2. Electronic and steric effects of a fluorine substituent on an adjacent π system.

In spite of their potential, however, studies of pinpoint-fluorinated PAHs have been hampered by the lack of available methods for their systematic synthesis [8]. Synthetic approaches to fluorinated aromatic compounds are broadly classified into two categories: (i) strategies for the introduction of fluorine (Scheme 1) and (ii) strategies for the construction of fluorinated rings. Although the regioselective introduction of fluorine into aromatic systems has been studied for a long time [9], it has drawbacks, namely, the need for the prior regioselective introduction of a functional group (a) or a directing group (b) to control the regioselectivity of the reaction, as well as the construction of the PAH skeleton. In spite of its efficiency, the construction of fluorinated aromatic rings has been limited to the oxidative photocyclization or the coupling reaction of *cis*-stilbene derivatives [10].



Scheme 1. Strategies for the Introduction of fluorine to form fluoroarenes (FG = functional group; DG = directing group).

By means of the latter strategy, we have reported the synthesis of pinpoint-fluorinated phenacenes by the cyclization of 1,1-difluoro-1-alkenes catalyzed by cationic Pd(II) species (Figure 3) [6]. 1,1-Difluoroalkenes **1**, possessing an *o*-biphenyl skeleton were treated with a catalytic amount of $[\text{Pd}(\text{MeCN})_4](\text{BF}_4)_2$ or $\text{PdCl}_2/\text{AgOTf}$ (1:2) in the presence of boron trifluoride etherate (1.0 equiv) in 1,1,1,3,3,3-hexafluoropropan-2-ol [11]. Pinpoint-monofluorinated chrysenes ([4]phenacenes) **2a** and **2b** and picenes ([5]phenacenes) **2c–e** were synthesized in good yields, although *difluorinated* PAHs have not yet been synthesized by this protocol.

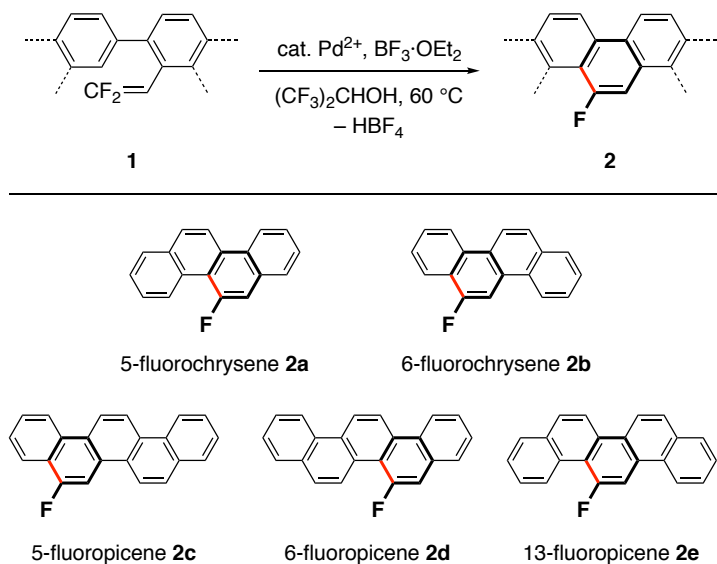


Figure 3. Strategy for the construction of fluorinated rings to form fluoroarenes: electrophilic activation of 1,1-difluoro-1-alkenes (synthesis of pinpoint-monofluorinated phenacenes).

In this paper, the syntheses of pinpoint-difluorinated PAHs involving the Pd(II)-catalyzed Friedel–Crafts-type cyclization of 1,1,2-trifluoro- and 1,1-difluoro-1-alkenes and the In(III)-catalyzed Friedel–Crafts-type cyclization of 1,1-difluoroallenes are described. The assembly of an array of difluorinated PAHs formed via these protocols and previously reported monofluorinated PAHs, which mainly comprised phenacenes, enabled studies of their physical properties such as solubility, downfield shift in ^{19}F NMR spectroscopy, and HOMO/LUMO energy gap.

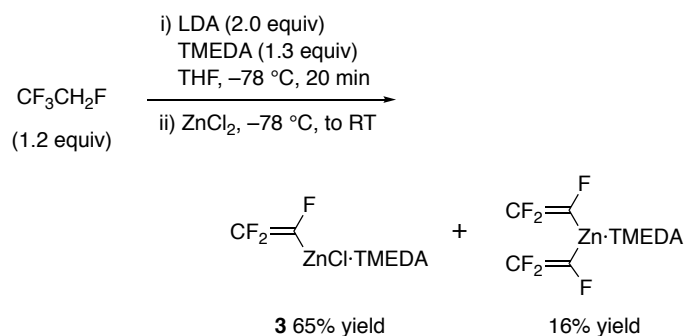
2. Results and discussion

2.1. Synthesis of *vic*-difluorinated PAHs

Although *vic*-difluorinated aromatic compounds constitute an attractive subfamily of pinpoint-fluorinated PAHs, their selective synthesis has been rare [12]. We envisioned that the employment of 1,1,2-trifluoro-1-alkenes as substrates for the aforementioned electrophilic cyclization (Friedel–Crafts-type cyclization) would enable the facile construction of *vic*-difluorinated PAHs.

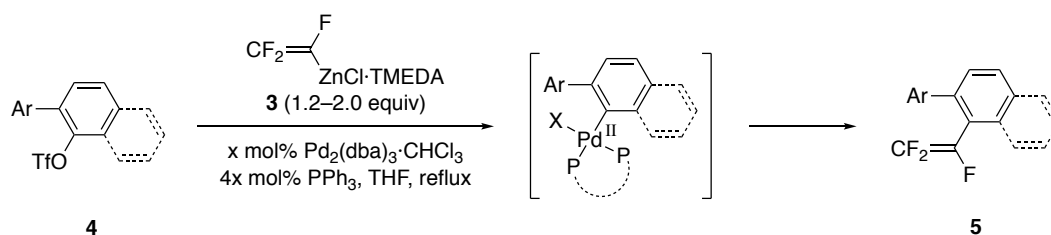
2.1.1. Preparation of 1,1,2-trifluoro-1-alkenes

The required 1,1,2-trifluoro-1-alkenes were prepared by the Negishi coupling of a trifluorovinylzinc(II) complex with the corresponding aryl triflates or iodides [13]: Trifluorovinyl lithium, which was generated from commercially available 1,1,1,2-tetrafluoroethane and LDA (2.0 equiv), was treated with zinc dichloride in the presence of TMEDA at $-78\text{ }^{\circ}\text{C}$ (Scheme 2). ^{19}F NMR analysis indicated that trifluorovinylzinc(II) chloride–TMEDA complex **3** (65% yield based on ZnCl_2) was obtained along with an inseparable bis(trifluorovinyl)zinc complex (16% yield).



Scheme 2. Preparation of trifluorovinylzinc(II) complex **3**.

The Negishi coupling of trifluorovinylzinc(II) complex **3** afforded the required 1,1,2-trifluoro-1-alkenes (Table 1). Trifluoroalkene **5a**, which bears a biphenyl moiety, was prepared from **3** and commercially available 2-iodo-1,1'-biphenyl in 98% yield (Entry 1). Aryl triflates **4b** and **4c** afforded the corresponding products **5b** and **5c** in 94% and 68% yields, respectively, using a 1,3-bis(diphenylphosphino)propane (dppp) ligand (Entries 2–5). The coupling of triflates **4d** and **4e** proceeded smoothly to afford **5d** and **5e** in 27% and 85% yields, respectively (Entries 6,7).

Table 1. Preparation of 1,1,2-trifluoro-1-alkenes.

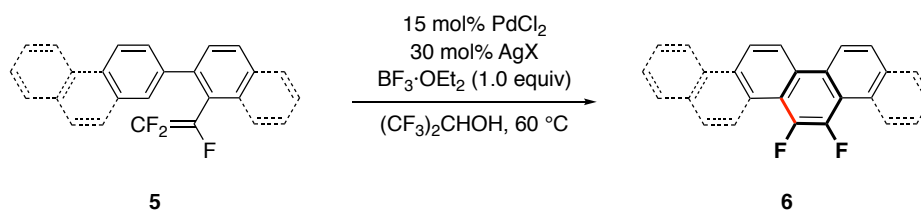
Entry	Triflate (Iodide)	Trifluoroalkene	x	t (h)	Yield (%) ^a	
1			5a	2	18	98
2			5b	10	11	8 ^b
3 ^c			5b	8	24	94
4			5c	10	19	20 ^b
5 ^c			5c	5	7	68
6			5d	10	25	27
7			5e	10	13	85

^a ¹⁹F NMR yield based on PhCF₃ as an internal standard. ^b Isolated yield. ^c Instead of PPh₃, dppp (2x mol%) was used. dba = benzylideneacetone.

2.1.2. Electrophilic cyclization of 1,1,2-trifluoro-1-alkenes

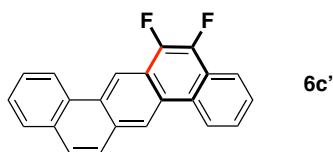
Having synthesized the required trifluoroalkenes, the Pd(II)-catalyzed electrophilic cyclization was examined (Table 2). The cyclization of trifluoroalkene **5a** proceeded under catalysis by PdCl₂/AgOTf [6a] to afford 9,10-difluorophenanthrene (**6a**) in 47% yield (Entry 1). Cyclization on the naphthalene moiety in **5b** proceeded to afford the product as a single isomer (51% yield, Entry 2). A ¹⁹F NMR study of the obtained product suggested that 5,6-difluorochrysene (**6b**) was obtained (*vide infra*). Thus, the cyclization reaction took place at the α-position of the naphthalene substructure, and the same regioselectivity was observed as in the cyclization of 1,1-difluoro-1-alkenes [6a]. The PdCl₂/AgNTf₂

catalytic system was effective for increasing the yield of **6**. *vic*-Difluorinated chrysene **6b** and picenes **6c/6c'** were synthesized from trifluoroalkenes **5b** and **5c** in 78% and 63% yields, respectively (Entries 3–5). As shown in Entry 6, it was revealed that cyclization on a benzene moiety was slower than on a naphthalene moiety. Phenylated trifluoroalkene **5d** afforded 5,6-difluorochrysene (**6b**) albeit only in 18% yield, which was much lower than that obtained by the reaction of naphthylated trifluoroalkene **5b** (78% yield, Entry 3). In other words, *vic*-difluorinated phenacenes were synthesized in greater yields by cyclization on a naphthalene or phenanthrene moiety rather than on a benzene moiety. The cyclization of trifluoroalkene **5e** successfully afforded difluorinated picene **6e** in 98% yield (Entry 8). The regiochemistry observed in the cyclization of **5b**, **5c**, and **5e** can be explained by a Friedel–Crafts-type mechanism (*vide infra*). Thus, it stems from the high reactivity of the α carbon of naphthalene and the C1 carbon of phenanthrene toward electrophilic aromatic substitution.

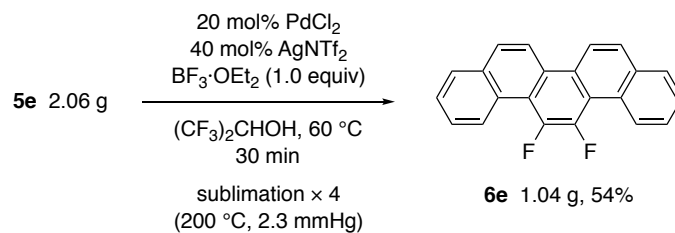
Table 2. Synthesis of *vic*-difluorophenacenes by electrophilic cyclization of 1,1,2-trifluoro-1-alkenes.^a

Entry	Trifluoroalkene	AgX	<i>t</i> (h)	Difluorophenacene	Yield (%)		
1		5a	AgOTf	2		6a	47
2		5b	AgOTf	2		6b	51 ^a
3		5b	AgNTf ₂	2		6b	78
4		5c	AgOTf	2.5		6c	27 ^{a,b}
5		5c	AgNTf ₂	2		6c	72 (6c : 6c' = 88 : 12) ^a 63 (6c : 6c' = 89 : 11)
6		5d	AgNTf ₂	2		6b	18 ^a
7		5e	AgOTf	1.3		6e	75 ^a
8		5e	AgNTf ₂	1.3		6e	98

^a ¹⁹F NMR yield based on PhCF₃ as an internal standard. ^b A small amount of **6c'** was observed by ¹⁹F NMR spectroscopy. Tf = trifluoromethanesulfonyl.



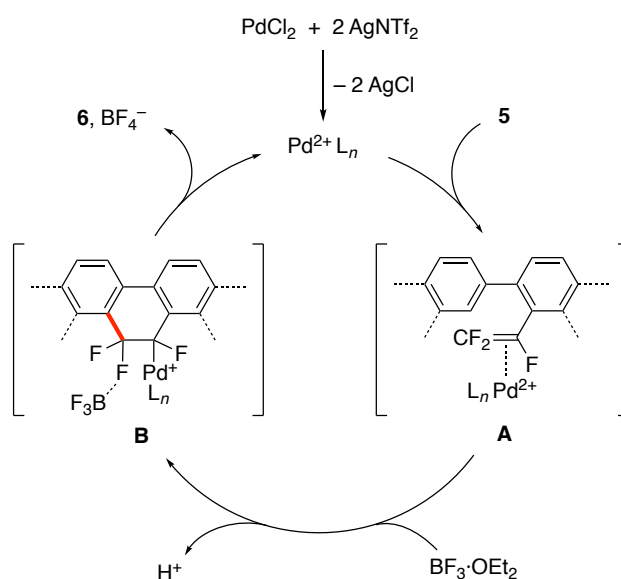
Electrophilic cyclization was also conducted in a gram-scale operation (Scheme 3). Trifluoroalkene **5e** (2.06 g) underwent cyclization in the presence of a PdCl₂/AgNTf₂ catalyst (20 mol%) to afford crude 13,14-difluoropicene (**6e**). Sublimation (200 °C, 2.3 mmHg, four cycles) gave pure **6e** in the form of yellow needles (1.04 g; 54% yield).



Scheme 3. Gram-scale synthesis of 13,14-difluoropicene (**6e**).

2.1.3. Catalytic cycle

A mechanism of the cyclization of 1,1,2-trifluoro-1-alkenes **5** is proposed in Scheme 4. Trifluoroalkenes **5** coordinate to the cationic palladium(II) center to form π -complexes **A**, in which the electron density of the trifluoroalkene moiety is lowered. This electrophilic activation promotes a Friedel–Crafts-type ring closure to provide cyclic alkylpalladium(II) intermediates **B**, which in turn undergo the BF_3 -assisted β -fluorine elimination to yield *vic*-difluorinated phenacenes **6**. The formation of BF_4^- ion regenerates the active cationic palladium(II) species.

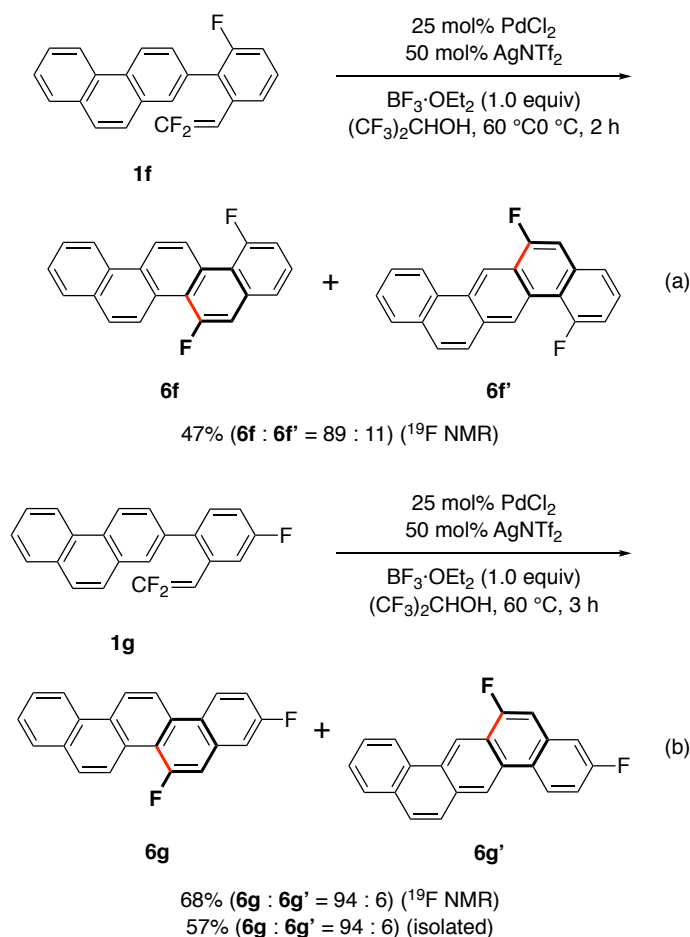


Scheme 4. Plausible mechanism for cyclization of trifluoroalkenes **5** ($\text{L} = \text{solvent}$).

2.2. Synthesis of other difluorinated PAHs

As well as *vic*-difluorinated phenacenes, other difluorophenacenes and related F-PAHs were synthesized by the cyclization of 1,1-difluoro-1-alkenes bearing a fluorophenyl group (Scheme 5). 1,1-

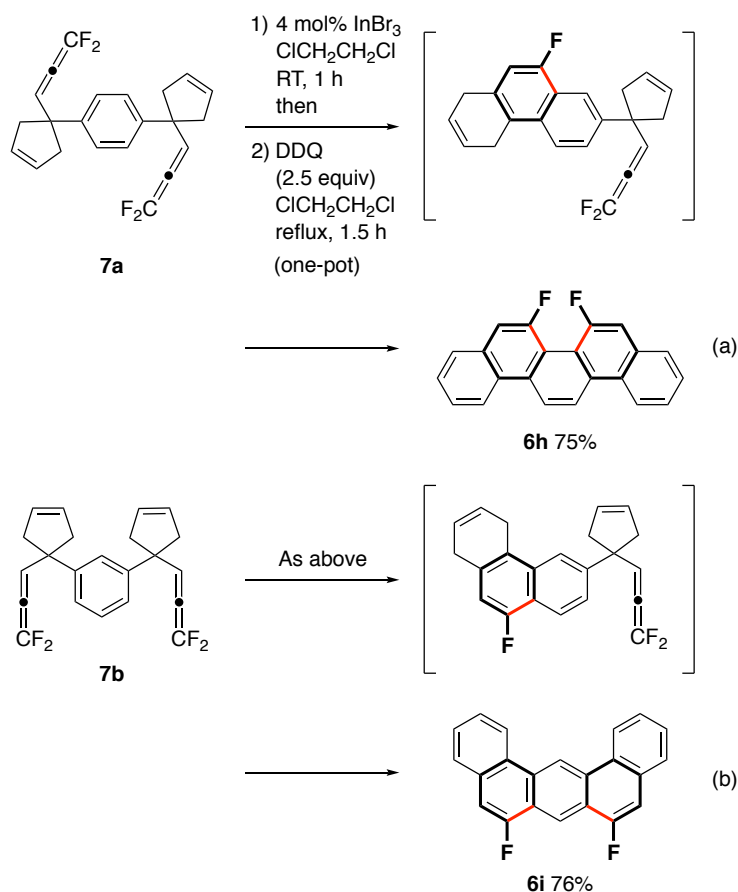
Difluoro-1-alkenes **1f** and **1g**, which bear an additional fluorine substituent on one of their aromatic rings, underwent cyclization under catalysis by cationic palladium(II) species to afford the corresponding difluoropicenes **6f/6f'** and **6g/6g'** in 47% and 68% yields, respectively.



Scheme 5. Synthesis of pinpoint-difluorinated picenes by electrophilic cyclization of 1,1-difluoro-1-alkenes.

Our established protocol for the cyclization/ring expansion of 1,1-difluoroallenes [14] was conducted in a tandem fashion to afford the desired non-*vic*-difluorinated PAHs. When bis(1,1-difluoroallene) **7a**, which was readily prepared from *p*-xylene, was subjected to catalysis by $InBr_3$, 6,7-difluoropicene (**6h**) was obtained as a single isomer in 75% yield (Scheme 6a). The dihydrophenanthrene intermediate generated in situ underwent a second cyclization reaction at the α -position of the newly formed naphthalene substructure, followed by one-pot dehydrogenation by DDQ

to give **6h**. Bis(1,1-difluoroallene) **7b**, which was prepared from *m*-xylene, also underwent tandem cyclization in a similar manner to afford difluorobenzanthracene **6i** as a single isomer in 76% yield (Scheme 6b). Severe steric repulsion probably promoted cyclization at the electronically less reactive β -position of the naphthalene substructure.

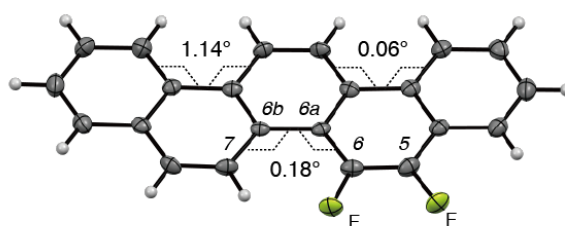


Scheme 6. Synthesis of pinpoint-difluorinated PAHs by tandem electrophilic cyclization of bis(1,1-difluoroallene)s.

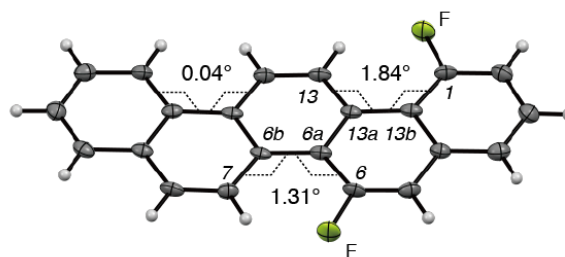
2.3. Planarity of pinpoint-fluorinated PAHs

Because of the low bulk of fluorine, in the same way as the reported monofluorinated **2a**, **2b**, **2d**, and **2e**, [6a] the pinpoint-difluorinated PAHs have planar structures (Figure 4). Single crystal X-ray structure analysis of 5,6-difluoropicene (**6c**, CCDC 1563733) indicated that this molecule has a C6–C6a–C6b–C7 torsion angle of 0.18°, which is smaller than that observed in the parent picene (1.96°, CCDC 991788). 1,6-Difluoropicene (**6f**, CCDC 1547302) has C1–C13b–C13a–C13 and C6–C6a–C6b–

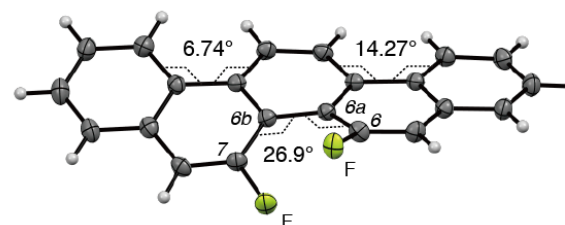
C7 torsion angles of 1.84° and 1.31° , respectively, which are similar to those in picene. These facts suggest that the planarity of the pinpoint-fluorinated PAHs was not affected by the introduction of fluorine [15]. As an exception, 6,7-difluoropicene (**6h**, CCDC 1545329) has a large C6–C6a–C6b–C7 torsion angle (26.9°), which is ascribed to the repulsive interaction between the two fluorine atoms.



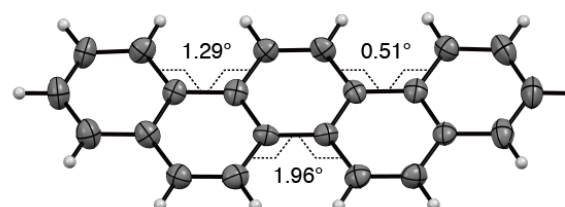
(a) 5,6-Difluoropicene (**6c**)



(b) 1,6-Difluoropicene (**6f**)



(c) 6,7-Difluoropicene (**6h**)



(d) Picene

Figure 4. ORTEP diagrams of pinpoint-difluorinated picenes.

2.4. Downfield shift in ^{19}F NMR signals of bay-region fluorine atoms

Chemical shifts in ^{19}F NMR spectroscopy are important parameters for characterizing the structures of fluorine-containing molecules. For the F-PAHs, the ^{19}F NMR signals of bay-region fluorine atoms were found to undergo a drastic downfield shift in comparison with those of non-bay-region (K-region, Figure 5) [1a,b] fluorine atoms.

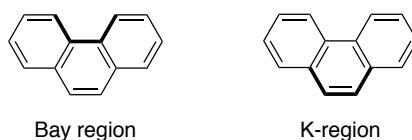


Figure 5. Bay- and K-regions of PAHs.

Single crystal X-ray structure analysis confirmed that 6-fluorochrysene (**2b**, CCDC 911876) [6a], a substituted 9-fluorophenanthrene (**2f**, CCDC 1058043) [6b], and 6-fluorodibenz[*a,h*]anthracene (**2g**, CCDC 978889) [6a] exhibited ^{19}F NMR signals at 38.4, 37.4, and 37.0 ppm, respectively (vs. C_6F_6 , Figure 6) [16]. 9-Fluorophenanthrene also exhibited a ^{19}F NMR signal at 37.9 ppm [17]. Thus, the signals of fluorine atoms located in the K-region were normally observed at 37–40 ppm (upfield region). 1-Fluoronaphthalene also exhibited a ^{19}F NMR signal in this region (39.1 ppm) [18].

In contrast, 5-fluorochrysene (**2a**, CCDC 911785) [6a], 6-fluoropicene (**2d**, CCDC 978888) [6a], 13-fluoropicene (**2e**, CCDC 957306) [6a], 1,6-difluoropicene (**6f**, CCDC 1547302), and 6,7-difluoropicene (**6h**, CCDC 1545329), in which the fluorine atoms are located in bay regions, exhibited ^{19}F NMR signals in the range of 50–56 ppm (downfield region).

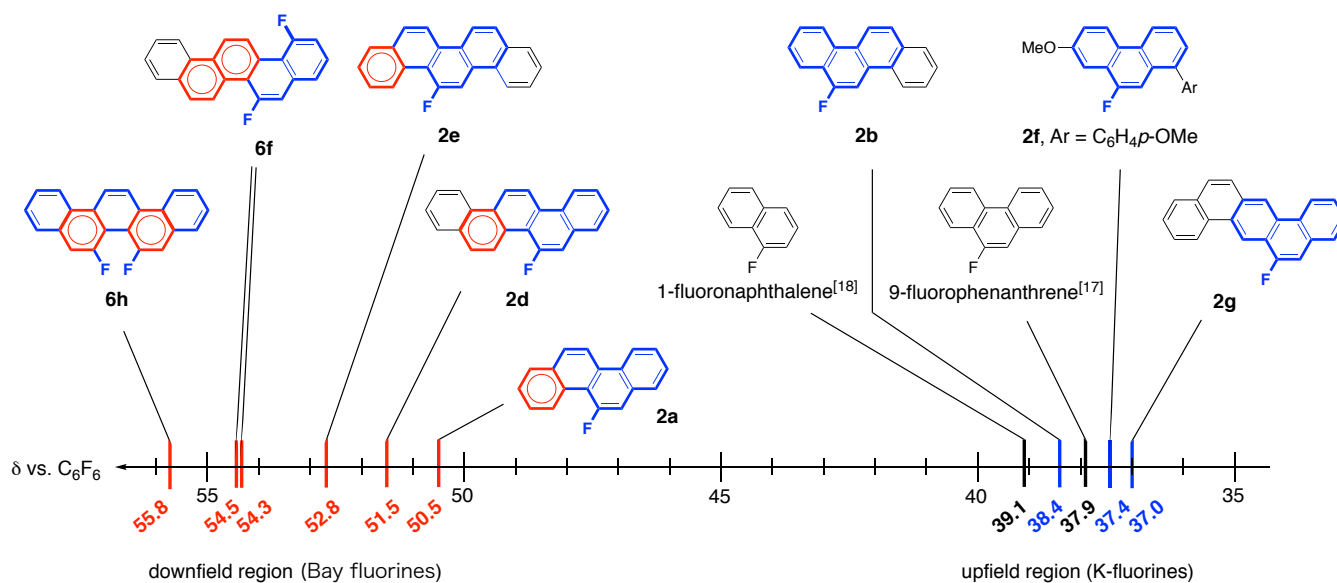


Figure 6. Colored: Structures and ^{19}F NMR chemical shifts (vs. C_6F_6) of F-PAHs, of which the structures were determined by single crystal X-ray structure analysis. Uncolored: Structures and chemical shifts (vs. C_6F_6) of F-PAHs in the literature.

It must be emphasized that the chemical shifts of the ^{19}F NMR signals for pinpoint-fluorinated PAHs **2c** [6a], **6g**, and **6i** were fully consistent with the rule described above (Figure 7). Therefore, their structures were determined not by single crystal X-ray structure analysis but by ^{19}F NMR. 5-Fluoropicene (**2c**) and difluorinated dibenzanthracene **6i** have fluorine substituents in the non-bay (K) region, of which the signals were observed in the upfield region (40.2 ppm for **2c** and 37.2 ppm for **6i**). Difluoropicene **6g** has a bay-region fluorine substituent (C6), of which the signal appeared as a doublet ($J_{\text{FH}} = 16$ Hz) in the downfield region (54.5 ppm). Although the non-bay-region fluorine atom of **6g** (C3) exhibited a signal that was apparently in the downfield region (49.5 ppm, dd), this was an acceptable value because the similar fluorine atom in 2-fluorophenanthrene exhibited a signal at 47.1 ppm [19].

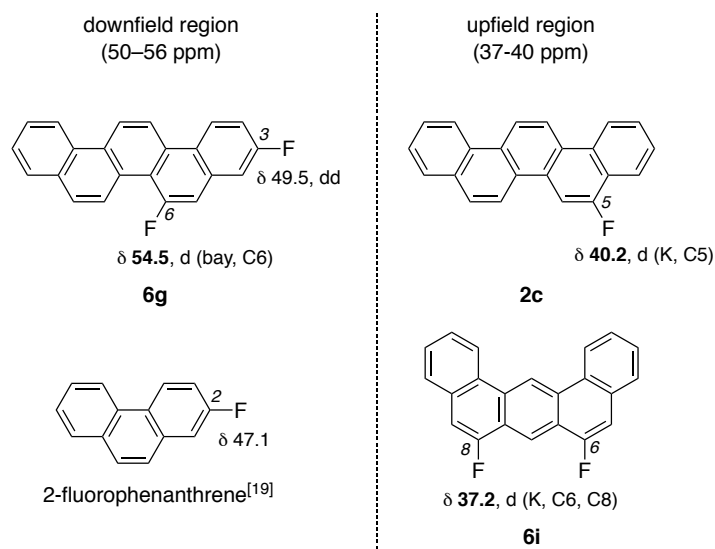
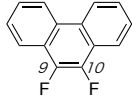
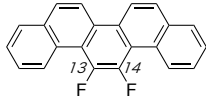
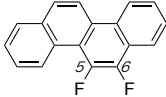
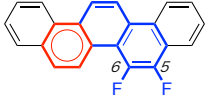


Figure 7. Structures and ^{19}F NMR assignments of **2c**, **6g**, and **6i** (vs. C_6F_6).

NMR signals of fluorine atoms in *vic*-difluorinated phenacenes appeared in distinct 21–24 ppm (downfield) and 10–13 ppm (upfield) regions (Table 3). 9,10-Difluorophenanthrene (**6a**), in which both fluorine atoms are in the non-bay (K) region, exhibited a ^{19}F NMR signal in the upfield region (10.4 ppm). On the other hand, 13,14-difluoropicene (**6e**), in which both fluorine atoms are in the bay region, exhibited a ^{19}F NMR signal in the downfield region (23.9 ppm). 5,6-Difluorochrysene (**6b**) and 5,6-difluoropicene (**6c**, CCDC 1563733), which both have one bay-region fluorine atom and one non-bay-region (K) fluorine atom, exhibited signals in both the downfield region (21.6 ppm for **6b** and 22.0 ppm for **6c**) and the upfield region (12.6 ppm for **6b** and 13.0 ppm for **6c**). On the basis of these observations, ^{19}F NMR signals of *vic*-difluorinated PAHs are observed in both downfield and upfield regions, and can reasonably be assigned to bay-region and non-bay-region (K) fluorine atoms, respectively.

Table 3. ^{19}F NMR chemical shifts (vs. C_6F_6) and assignments of *vic*-difluorinated phenacenes. ^a

Compounds	Downfield region (δ 21–24)	Upfield region (δ 10–13)
	6a	10.4 (K, C9, C10)
	6e	23.9 (bay, C13, C14)
	6b	21.6 (bay, C5) 12.6 (K, C6)
	6c	22.0 (bay, C6) 13.0 (K, C5)

^a Colored: Structure determined by single crystal X-ray structure analysis.

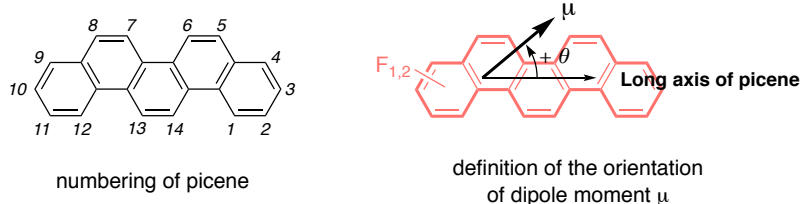
The abovementioned downfield shifts were apparently due to the deshielding effect of the opposite benzene ring in the bay region, whereas systematic study on the deshielding effect has not been reported till date [10i]. In the array of synthesized pinpoint-fluorinated PAHs, a downfield shift was observed in all the ^{19}F NMR signals of bay-region fluorine atoms. The magnitudes of the downfield shifts were ca. 11–19 ppm for the monofluorinated and the non-*vic*-difluorinated PAHs and ca. 8–14 ppm for the *vic*-difluorinated PAHs.

2.5. Polarity, solubility, and mobility of pinpoint-fluorinated picenes

A fluorine substituent has an electron-withdrawing inductive effect, and its lone pairs are involved in a repulsive interaction with the adjacent π -electrons (Figure 2), which leads to the polarization of the molecule. In fact, theoretical calculations indicated that polarity was induced in the phenacene molecules (Table 4). For example, the dipole moments of 5- and 6-fluoropicenes are 1.37 and 1.28 D (Entries 2 and 3), respectively, whereas picene has a dipole moment of 0.06 D (Entry 1). Thus, the introduction of fluorine substituent(s) effectively induced the polarization of the PAH molecules.

Wet processes (solution processes) are promising methods that enable the low-cost and easy fabrication of electronic devices and are characteristically employed with organic materials. For the adoption of these processes, the solubility of semiconducting materials in organic solvents is an important factor. Recently, we reported on the solubilizing effect of the introduction of the fluorine atoms into aromatic systems. However, no systematic study of this effect has been conducted to date [6a]. We therefore investigated the solubilities of the pinpoint-fluorinated PAHs.

The solubilities of the pinpoint-fluorinated picenes and picene in THF were measured via the Lambert–Beer law, using a UV–vis spectrometer. Among the monofluorinated picenes, 6-fluoropicene exhibited high solubility in THF (**2d**, 0.16 mol/L, 5.3 wt%, Entry 3), which represents a 25-fold increase in comparison with picene (Entry 1). 13-Fluoropicene also exhibited high solubility (**2e**, 15-fold increase with respect to picene, Entry 4). Among the difluorinated picenes, 1,6-difluoropicene (**6f**, 0.081 mol/L, 2.9 wt%, Entry 7) exhibited comparable solubility to 13-fluoropicene (**2e**, Entry 4), which was 13 times that of picene. 6,7-Difluoropicene also exhibited high solubility (**6h**, 0.15 mol/L, 5.4 wt%, Entry 9). It is noteworthy that 5-fluoropicene (**2c**) exhibited p-type semiconducting behavior (mobility $2.81 \times 10^{-5} \text{ cm}^2/\text{Vs}$) [20].

Table 4. Solubility of pinpoint-fluorinated picenes in THF.

Entry	Compound	λ_{\max} (nm)	ϵ at λ_{\max} (10^5 L/mol cm)	Solubility		Dipole moment (debye), θ ($^\circ$)	
				(10^{-2} mol/L) ^a	(wt%)		
1	picene	–	285	1.02	0.64 (1) [6a]	0.20	0.06, 90
2	5-fluoropicene	2c	285	1.03	1.4 (2) [6a]	0.48	1.37, 69
3	6-fluoropicene	2d	287	1.07	16 (25) [6a]	5.3	1.28, 102
4	13-fluoropicene	2e	282	0.66	9.3 (15) [6a]	3.1	1.14, –113
5	5,6-difluoropicene	6c	287	1.24	3.9 (6)	1.4	2.40, 84
6	13,14-difluoropicene	6e	282	1.25	2.8 (4)	0.98	2.07, –90
7	1,6-difluoropicene	6f	286	1.16	8.1 (13)	2.9	0.55, 165
8	3,6-difluoropicene	6g	285	1.10	5.0 (8)	1.8	1.85, 42
9	6,7-difluoropicene	6h	290	0.98	15 (23)	5.4	2.54, 90

^a The relative solubility is indicated in parentheses.

The introduction of fluorine substituents into organic molecules has been practiced for a long time in the life sciences [3d]. Fluorine substituents often improve the bioactivity of the original molecule because of their electronic effects and low steric demand. Our study clearly demonstrated that the introduction of one or two fluorine atoms into PAHs had an advantageous effect on their solubility without affecting their planarity, which is of particular interest in materials science [21].

2.6. HOMO and LUMO energy levels of pinpoint-fluorinated picenes

The energy levels of molecules are important factors in the development of electronic devices with high carrier mobility. In addition, the HOMO energy level is a key parameter used to estimate the resistance of materials to aerial oxidation. Thus, the HOMO and LUMO energy levels were systematically investigated for the pinpoint-fluorinated picenes that we synthesized.

The energy levels of the pinpoint-fluorinated picenes are listed in Table 5. The energy gaps (E_g s) of the pinpoint-fluorinated picenes and picene were determined on the basis of the longest absorption wavelength (λ_{offset}). Picene (i.e., [5]phenacene) exhibited an energy gap of 3.71 eV (Entry 1), which was smaller than that of chrysene (i.e.; [4]phenacene, 3.8 eV) [22]. Pinpoint-fluorinated picenes **2c–e**, **6c**, and **6e–g** exhibited E_g values of 3.61–3.69 eV (Entries 2–8), which displayed correlations with those calculated by DFT (B3LYP/6–31G*, Figure 8). 6,7-Difluoropicene (**6h**) exhibited the lowest E_g value of 3.45 eV (Entry 9). The introduction of fluorine thus lowered the energy gaps of the picenes.

The reduction peaks of the pinpoint-fluorinated picenes were not definite in cyclic voltammograms (CV). The HOMO and LUMO energy levels of these compounds were therefore determined by differential pulse voltammetry (DPV). The oxidation peak (E_{OX}) observed in the corresponding differential pulse voltammogram indicated that picene has a deeper HOMO level (–5.62 eV, Entry 1) than pentacene (–5.1 eV) and TIPS-pentacene (–5.1 eV) [23]. The HOMO levels of the pinpoint-fluorinated picenes, which were estimated in a similar manner, range from –5.72 to –5.84 eV (Entries 2–9). Substitution by fluorine thus lowered the HOMO levels of the picenes by 0.10–0.22 eV. These observations are consistent with the fact that the HOMO levels of picene and 13-fluoropicene (**2e**), estimated by ultraviolet photoelectron spectroscopy (UPS), are –5.3 eV and –5.4 eV, respectively (Entries 1 and 4). The deeper HOMO levels of the pinpoint-fluorinated picenes contribute to the high resistance of these compounds to aerial oxidation.

Reduction peaks could not be found in the differential pulse voltammograms because of overlaps with the solvent signals. The LUMO levels of the pinpoint-fluorinated picenes were therefore determined by the equation $E_{\text{LUMO}} = E_{\text{HOMO}} + E_g$. The LUMO energy levels of the fluorinated picenes range from –2.32 to –2.03 eV, which are lower than that of picene (–1.91 eV) by 0.12–0.41 eV.

Table 5. HOMO and LUMO energy levels of pinpoint-fluorinated picenes.

Entry	Compound		λ_{offset} (nm)	E_g (eV) ^a	$E_{\text{LUMO}} - E_{\text{HOMO}}$ (eV, calcd.) ^b	E_{OX} (V) ^c	E_{HOMO} (eV) ^{d,e}	E_{LUMO} (eV) ^{e,f}
1	picene	–	335	3.71	4.22	0.82	–5.62 –5.3 ^g	–1.91
2	5-fluoropicene	2c	336	3.69	4.20	0.92	–5.72 (–0.10)	–2.03 (–0.12)
3	6-fluoropicene	2d	342	3.63	4.11	0.92	–5.72 (–0.10)	–2.09 (–0.18)
4	13-fluoropicene	2e	338	3.68	4.13	0.95	–5.75 (–0.13) –5.4 ^g	–2.07 (–0.16)
5	5,6-difluoropicene	6c	341	3.65	4.09	0.96	–5.76 (–0.14)	–2.12 (–0.21)
6	13,14-difluoropicene	6e	342	3.63	4.07	1.01	–5.81 (–0.19)	–2.18 (–0.27)
7	1,6-difluoropicene	6f	344	3.61	4.07	1.04	–5.84 (–0.22)	–2.23 (–0.32)
8	3,6-difluoropicene	6g	340	3.65	4.11	0.98	–5.78 (–0.16)	–2.13 (–0.22)
9	6,7-difluoropicene	6h	360	3.45	4.01	0.97	–5.77 (–0.15)	–2.32 (–0.41)

^a $E_g / \text{eV} = 1240 / (\lambda_{\text{offset}} / \text{nm})$. ^b Calculated using the B3LYP/6–31G* basis set. ^c Working/counter electrodes: Pt, reference electrode: Ag/Ag⁺, *n*-Bu₄N ClO₄, vs. Fc/Fc⁺. ^d $E_{\text{HOMO}} / \text{eV} = -4.80 - E_{\text{OX}} / \text{eV}$. ^e The decrease with respect to picene is indicated in parentheses. ^f $E_{\text{LUMO}} = E_{\text{HOMO}} + E_g$. ^g Based on the ionization potential determined by UPS measurements [6a].

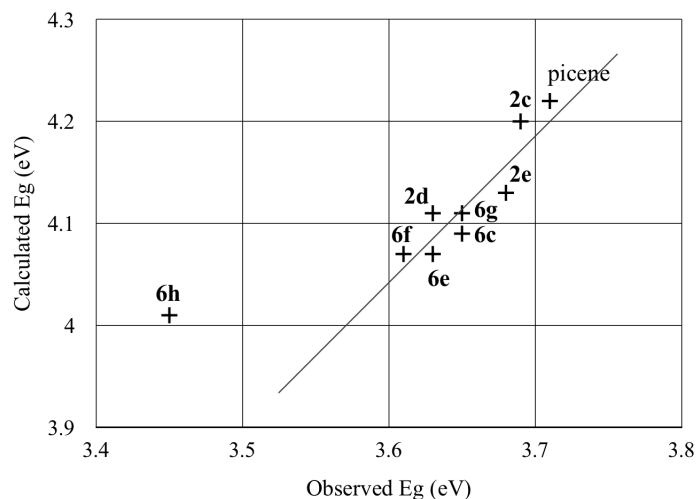


Figure 8. Comparison of the observed and calculated energy gaps of the pinpoint-fluorinated picenes and picene.

3. Conclusions

An array of pinpoint-fluorinated PAHs was successfully prepared by the electrophilic cyclization of 1,1,2-trifluoro-1-alkenes or 1,1-difluoro-1-alkenes catalyzed by cationic Pd(II) species or by the In(III)-catalyzed tandem cyclization of bis(1,1-difluoroallene)s. We thus, gained a broader perspective on their physical properties. (i) Single crystal X-ray structure analysis and ^{19}F NMR spectroscopy showed that the NMR signals of the bay-region fluorine atoms shifted downfield by ca. 11–19 ppm (monofluorinated and non-*vic*-difluorinated PAHs) or by ca. 8–14 ppm (*vic*-difluorinated PAHs). (ii) A study of the solubility revealed that the introduction of fluorine into PAH molecules solubilizes them in organic solvents, and 6-fluoropicene and 6,7-difluoropicene exhibited the highest solubilities in THF (5.3 and 5.4 wt%). In addition, 5-fluoropicene exhibited p-type semiconducting behavior ($2.81 \times 10^{-5} \text{ cm}^2/\text{Vs}$). (iii) UV-vis spectroscopy and DPV indicated that the energy gaps (E_g s) of the pinpoint-fluorinated PAHs are smaller (3.61–3.69 eV) than that of the fluorine-free PAH (i.e., picene) and that the HOMO (–5.72 to –5.84 eV) and LUMO (–2.32 to –2.03 eV) energy levels of the pinpoint-fluorinated picenes were lowered by 0.10–0.22 eV and 0.12–0.41 eV, respectively.

4. Experimental

4.1. General information

IR spectra were recorded on a Horiba FT-300S spectrometer. NMR spectra were recorded on a Bruker Avance 500 spectrometer in CDCl₃, at 500 MHz (¹H NMR), at 126 MHz (¹³C NMR), and at 470 MHz (¹⁹F NMR). Chemical shift values were given in ppm relative to internal Me₄Si (for ¹H NMR: δ = 0.00), CDCl₃ (for ¹³C NMR: δ = 77.0), and C₆F₆ (for ¹⁹F NMR: δ = 0.0) [16]. Mass spectra were taken with Jeol JMS-T100GCV (EI, 70 eV) or JMS-T100CS (APCI⁺) spectrometers. UV–Vis absorption spectra were determined using a Jasco V-630 spectrometer. Cyclic and differential pulse voltammograms were recorded with a BAS ALS 600Bz analyser. Elemental analyses were performed with a Yanako MT-3 CHN Corder apparatus. Mobility was measured using a Keysight 4156C semiconductor parameter analyser.

4.2. Synthesis of *vic*-difluorinated PAHs

4.2.1. Preparation of 1,2,2-trifluorovinylzinc(II) chloride–TMEDA (1/1) (**3**)

Trifluorovinylzinc(II) chloride–TMEDA complex was prepared by the method in the literature but at –78 °C [13c]. To a THF solution (7 mL) of 1,1,1,2-tetrafluoroethane [gas (300 mL) was condensed at –78 °C, 13.5 mmol] and TMEDA (2.20 mL, 14.7 mmol) was slowly added a THF solution (11 mL) of lithium diisopropylamide (LDA, 22.6 mmol) at –78 °C over 20 min. A THF solution (7 mL) of anhydrous ZnCl₂ (1.6 mol/L, 11.2 mmol) [24] was added to the reaction mixture at –78 °C. After stirring at –78 °C for 2 h, the reaction mixture was slowly warmed to room temperature. ¹⁹F NMR analysis of the colorless solution, using PhCF₃ as an internal standard, indicated that the desired trifluorovinylzinc(II)–TMEDA complex **3** was generated in 65% yield, along with 16% yield of divinylzinc(II) complex. This solution was kept in a refrigerator (–35 °C) without substantial decomposition over one month.

4.2.2. Preparation of biaryl triflates **4**

Biaryl triflate **4d** was prepared from phenylboronic acid and 2-bromo-1-trifluoromethanesulfonyloxynaphthalene under Pd catalysis [6a]. Other biaryl triflates were prepared

from the corresponding boronic acids and bromotriflates by a similar procedure. Specifically, phenanthren-2-ylboronic acid for **4c** was prepared from 2-bromophenanthrene [25] (*n*-BuLi 1.1 equiv, THF, $-90\text{ }^{\circ}\text{C}$; B(OMe)₃ 2.5 equiv, RT; aq. HCl, 98% yield).

4.2.3. Spectral data of biaryl triflates **4**

4.2.3.1. 2-(2-Naphthyl)phenyl trifluoromethanesulfonate (**4b**)

¹H NMR (500 MHz, CDCl₃): δ 7.29–7.35 (m, 3H), 7.38–7.43 (m, 2H), 7.44–7.49 (m, 2H), 7.74–7.79 (m, 2H), 7.81 (d, *J* = 8.5 Hz, 1H), 7.84 (s, 1H); ¹³C NMR (126 MHz, CDCl₃): 118.3 (q, *J*_{CF} = 321 Hz), 122.1, 126.4, 126.6, 126.9, 127.7, 128.15, 128.19, 128.5, 128.7, 129.0, 132.2, 132.8, 133.0, 133.2, 135.4, 146.9; ¹⁹F NMR (470 MHz, CDCl₃): δ 88.9 (s); IR (neat): $\tilde{\nu}$ 1419, 1203, 1136, 1093, 887, 729, 596 cm⁻¹; HRMS (70 eV, EI): *m/z* calcd. for C₁₇H₁₁F₃O₃S ([M]⁺): 352.0381; found: 352.0373.

4.2.3.2. 2-(Phenanthren-2-yl)phenyl trifluoromethanesulfonate (**4c**)

¹H NMR (500 MHz, CDCl₃): δ 7.42–7.51 (m, 3H), 7.59–7.64 (m, 2H), 7.67 (ddd, *J* = 7.1, 7.0, 1.5 Hz, 1H), 7.75 (d, *J* = 8.6, 2.0 Hz, 1H), 7.76 (d, *J* = 8.9 Hz, 1H), 7.78 (d, *J* = 9.0 Hz, 1H), 7.90 (dd, *J* = 7.9, 1.2 Hz, 1H), 7.99 (d, *J* = 1.9 Hz, 1H), 8.70 (d, *J* = 8.2 Hz, 1H), 8.75 (d, *J* = 8.6 Hz, 1H); ¹³C NMR (126 MHz, CDCl₃): 118.3 (q, *J*_{CF} = 321 Hz), 122.2, 122.8, 123.0, 126.79, 126.87, 126.92, 127.5, 127.6, 128.61, 128.63, 129.1, 129.3, 130.0, 132.0, 132.25, 132.31, 133.7, 135.2, 146.9; ¹⁹F NMR (470 MHz, CDCl₃): δ 88.3 (s); IR (neat): $\tilde{\nu}$ 1419, 1207, 1138, 906, 879, 742, 600 cm⁻¹; HRMS (70 eV, EI): *m/z* calcd. for C₂₁H₁₃F₃O₃S ([M]⁺): 402.0537; found: 402.0532.

4.2.3.3. 2-(2-Naphthyl)naphthalen-1-yl trifluoromethanesulfonate (**4e**)

¹H NMR (500 MHz, CDCl₃): δ 7.53–7.57 (m, 2H), 7.61–7.69 (m, 3H), 7.71 (ddd, *J* = 8.3, 7.0, 1.2 Hz, 1H), 7.89–7.94 (m, 2H), 7.94–7.99 (m, 3H), 8.05 (d, *J* = 1.5 Hz, 1H), 8.22 (d, *J* = 8.5 Hz, 1H); ¹³C NMR (126 MHz, CDCl₃): δ 118.1 (q, *J*_{CF} = 320 Hz), 121.7, 126.5, 126.7, 127.21, 127.24, 127.5, 127.8, 128.0, 128.1, 128.2, 128.3, 128.6, 128.7, 129.2, 132.7, 132.9, 133.3, 133.7, 134.1, 142.1; ¹⁹F NMR (470 MHz, CDCl₃): δ 87.7 (s); IR (neat): $\tilde{\nu}$ 3059, 1415, 1209, 1134, 816, 744 cm⁻¹; EA: calcd. for C₂₁H₁₃F₃O₃S: C 62.68%, H 3.26%; found: C 63.03%, H 3.25%.

4.2.4. Negishi-coupling of trifluorovinylzinc(II) chloride–TMEDA complex **3** with aryl iodides or triflates

4.2.4.1. Synthesis of 1,1,2-trifluoro-1-alkene **5a**

The reagent loading of **3** for the Negishi coupling was calculated on the basis of the concentration of **3** determined by ^{19}F NMR. Although the bis(trifluorovinyl)zinc complex partly took part in the coupling reaction [26], the amount of the bis(trifluorovinyl)zinc complex was excluded in the preparation of **5**.

To a THF solution (150 mL) of trifluorovinylzinc(II) **3** (0.126 mol/L, 18.9 mmol) were added 2-iodo-1,1'-biphenyl (4.44 g, 15.9 mmol), $\text{Pd}_2(\text{dba})_3 \cdot \text{CHCl}_3$ (392 mg, 0.378 mmol), and PPh_3 (426 mg, 1.61 mmol). The resulting solution was refluxed for 18 h. The reaction mixture was cooled to room temperature and silica gel was added. After removal of the solvent under reduced pressure, the residue was purified by column chromatography on silica gel (hexane) to give a dark red oil. This crude product was purified by Kügel–Rohr distillation to give trifluoroalkene **5a** as a colorless liquid (3.65 g, 98% yield).

4.2.4.2. Synthesis of 1,1,2-trifluoro-1-alkenes **5b–f**

Preparation of trifluoroalkene **5b** is described as a typical procedure. To a THF solution (83 mL) of **3** (0.143 mol/L, 11.9 mmol) were added triflate **4b** (2.10 g, 5.97 mmol), $\text{Pd}_2(\text{dba})_3 \cdot \text{CHCl}_3$ (502 mg, 0.485 mmol), and dppp (396 mg, 0.959 mmol). The resulting solution was refluxed for 24 h. The reaction mixture was cooled to room temperature and silica gel was added. After removal of the solvent under reduced pressure, the residue was purified by column chromatography on silica gel (hexane) to give trifluoroalkene **5b** as a yellow liquid (1.60 g, 94% yield).

4.2.5. Spectral data of 1,1,2-trifluoro-1-alkenes **5**

4.2.5.1. 2-(1,2,2-Trifluoroethenyl)-1,1'-biphenyl (**5a**)

^1H NMR (500 MHz, CDCl_3): δ 7.35–7.44 (m, 7H), 7.48–7.53 (m, 2H); ^{13}C NMR (126 MHz, CDCl_3): 125.0 (dd, $J_{\text{CF}} = 20, 4$ Hz), 127.4, 127.59, 127.60 (ddd, $J_{\text{CF}} = 219, 52, 20$ Hz), 128.3, 130.4, 130.4, 130.5, 130.7, 140.2, 142.7, 152.9 (ddd, $J_{\text{CF}} = 328, 277, 51$ Hz); ^{19}F NMR (470 MHz, CDCl_3): δ 3.77 (dd, $J =$

117, 30 Hz, 1F), 45.3 (dd, $J = 117, 74$ Hz, 1F), 60.8 (dd, $J = 74, 30$ Hz, 1F); IR (neat): $\tilde{\nu}$ 1782, 1284, 1138, 982, 741, 698 cm^{-1} ; HRMS (70 eV, EI): m/z calcd. for $\text{C}_{14}\text{H}_9\text{F}_3$ ($[\text{M}]^+$): 234.0656; found: 234.0656.

4.2.5.2. 1-(2-Naphthyl)-2-(1,2,2-trifluoroethenyl)benzene (**5b**)

^1H NMR (500 MHz, CDCl_3): δ 7.46 (dd, $J = 7.0, 7.0$ Hz, 1H), 7.49–7.57 (m, 6H), 7.83–7.90 (m, 4H); ^{13}C NMR (126 MHz, CDCl_3): 125.2 (dd, $J_{\text{CF}} = 20, 4$ Hz), 126.2, 126.3, 126.5, 127.3, 127.4, 127.6 (ddd, $J_{\text{CF}} = 233, 52, 20$ Hz), 127.7, 128.0, 128.2, 130.5, 130.7 (d, $J_{\text{CF}} = 2$ Hz), 130.8, 132.6, 133.3, 137.7, 142.5, 152.9 (ddd, $J_{\text{CF}} = 328, 278, 50$ Hz); ^{19}F NMR (470 MHz, CDCl_3): δ 2.95 (dd, $J = 117, 30$ Hz, 1F), 44.7 (dd, $J = 117, 74$ Hz, 1F), 60.2 (dd, $J = 74, 30$ Hz, 1F); IR (neat): $\tilde{\nu}$: 1778, 1491, 1284, 1138, 982, 820, 758 cm^{-1} ; HRMS (70 eV, EI): m/z calcd. for $\text{C}_{18}\text{H}_{11}\text{F}_3$ ($[\text{M}]^+$): 284.0813; found: 284.0806.

4.2.5.3. 1-(Phenanthren-2-yl)-2-(1,2,2-trifluoroethenyl)benzene (**5c**)

1.19 g, 68% yield, a pall yellow solid; ^1H NMR (500 MHz, CDCl_3): δ 7.43–7.47 (m, 1H), 7.54–7.57 (m, 3H), 7.60 (dd, $J = 7.4, 7.4$ Hz, 1H), 7.64–7.69 (m, 2H), 7.74 (d, $J = 9.0$ Hz, 1H), 7.77 (d, $J = 9.0$ Hz, 1H), 7.88–7.91 (m, 2H), 8.70 (dd, $J = 8.7, 8.7$ Hz, 2H); ^{13}C NMR (126 MHz, CDCl_3): 122.7, 122.8, 125.2 (dd, $J_{\text{CF}} = 20, 5$ Hz), 126.7, 126.8, 126.9, 127.4, 127.5, 127.7 (ddd, $J_{\text{CF}} = 222, 52, 20$ Hz), 128.1, 128.6, 129.6, 130.1, 130.5, 130.76, 130.77, 130.83, 132.0, 132.2, 138.4, 142.3, 152.9 (ddd, $J_{\text{CF}} = 328, 278, 50$ Hz); ^{19}F NMR (470 MHz, CDCl_3): δ 3.91 (dd, $J = 117, 30$ Hz, 1F), 45.6 (dd, $J = 117, 74$ Hz, 1F), 61.1 (dd, $J = 74, 30$ Hz, 1F); IR (neat): $\tilde{\nu}$ 1774, 1444, 1281, 1136, 980, 808, 742 cm^{-1} ; HRMS (70 eV, EI): m/z calcd. for $\text{C}_{22}\text{H}_{13}\text{F}_3$ ($[\text{M}]^+$): 334.0969; found: 334.0962.

4.2.5.4. 2-Phenyl-1-(1,2,2-trifluoroethenyl)naphthalene (**5d**)

0.464 g, 27% yield, a yellow liquid. ^1H NMR (500 MHz, CDCl_3): δ 7.39–7.49 (m, 5H), 7.56 (d, $J = 8.3$ Hz, 1H), 7.57 (d, $J = 6.3$ Hz, 1H), 7.64 (ddd, $J = 8.2, 7.0, 1.3$ Hz, 1H), 7.93 (d, $J = 8.2$ Hz, 1H), 8.02–8.06 (m, 2H); ^{13}C NMR (126 MHz, CDCl_3): 120.9 (dd, $J_{\text{CF}} = 19, 4$ Hz), 125.0, 125.5 (ddd, $J_{\text{CF}} = 234, 54, 20$ Hz), 126.5, 127.6, 127.7, 127.8, 128.3, 128.9, 131.45, 131.47, 132.55 (d, $J_{\text{CF}} = 1$ Hz), 132.63 (d, $J_{\text{CF}} = 3$ Hz), 140.3, 143.0, 153.4 (ddd, $J_{\text{CF}} = 327, 276, 51$ Hz); ^{19}F NMR (470 MHz, CDCl_3): δ 8.81 (dd, $J = 118, 27$ Hz, 1F), 46.9 (dd, $J = 118, 73$ Hz, 1F), 61.0 (dd, $J = 73, 27$ Hz, 1F); IR (neat): $\tilde{\nu}$ 1788, 1230,

1140, 1099, 947, 762, 702 cm^{-1} ; HRMS (70 eV, EI): m/z calcd. for $\text{C}_{18}\text{H}_{11}\text{F}_3$ ($[\text{M}]^+$): 284.0813; found: 284.0825.

4.2.5.5. 2-(2-Naphthyl)-1-(1,2,2-trifluoroethenyl)naphthalene (**5e**)

0.141 g, 85% yield, colorless crystals; ^1H NMR (500 MHz, CDCl_3): δ 7.54 (d, $J = 6.1$ Hz, 1H), 7.55 (d, $J = 6.1$ Hz, 1H), 7.60 (dd, $J = 7.5, 7.5$ Hz, 2H), 7.66 (dd, $J = 8.2, 8.2$ Hz, 2H), 7.89–7.97 (m, 5H), 8.07 (d, $J = 8.3$ Hz, 2H); ^{13}C NMR (126 MHz, CDCl_3): δ 121.1 (dd, $J_{\text{CF}} = 19, 4$ Hz), 125.0, 125.4 (ddd, $J_{\text{CF}} = 234, 54, 21$ Hz), 126.36, 126.38, 126.6, 126.9, 127.5 (d, $J_{\text{CF}} = 24$ Hz), 127.7, 127.8, 127.88, 127.92, 128.0, 128.29, 128.32, 131.5 (d, $J_{\text{CF}} = 3$ Hz), 132.6, 132.7, 133.2, 137.8, 142.8, 153.5 (ddd, $J_{\text{CF}} = 292, 276, 51$ Hz); ^{19}F NMR (470 MHz, CDCl_3): δ 8.64 (dd, $J = 118, 27$ Hz, 1F), 47.0 (dd, $J = 118, 72$ Hz, 1F), 61.2 (dd, $J = 72, 27$ Hz, 1F); IR (neat): $\tilde{\nu}$ 2924, 1790, 1300, 1138, 1095, 820, 746 cm^{-1} ; HRMS (70 eV, EI): m/z calcd. for $\text{C}_{22}\text{H}_{13}\text{F}_3$ ($[\text{M}]^+$): 334.0970; found: 334.0969.

4.2.6. Synthesis of *vic*-difluorinated PAHs **6a–e**

Synthesis of 5,6-difluorochrysene (**6b**) is described as a typical procedure. To a HFIP suspension (2 mL) of palladium(II) chloride (3.3 mg, 0.019 mmol) were added trifluoroalkene **5b** (57 mg, 0.20 mmol), silver bis(trifluoromethanesulfonyl)imide (23 mg, 0.059 mmol), and boron trifluoride etherate ($\text{BF}_3 \cdot \text{OEt}_2$, 25 μL , 0.20 mmol) at 0 $^\circ\text{C}$. After the reaction mixture was stirred for 2 h at 60 $^\circ\text{C}$, aqueous sodium hydrogen carbonate was added to quench the reaction. Organic materials were extracted with dichloromethane four times. The combined extracts were washed with brine and dried over anhydrous sodium sulfate. After removal of the solvent under reduced pressure, the residue was purified by column chromatography on silica gel (hexane) to give 5,6-difluorochrysene (**6b**) as colorless crystals (42 mg, 78% yield).

4.2.7. Spectral data of *vic*-difluorinated PAHs **6a–e**

4.2.7.1. 9,10-Difluorophenanthrene (**6a**)

0.100 g, 47% yield, a colorless solid; ^1H NMR (500 MHz, CDCl_3): δ 7.64–7.74 (m, 4H), 8.14–8.20 (m, 2H), 8.60–8.67 (m, 2H); ^{13}C NMR (126 MHz, CDCl_3): 120.9 (dd, $J_{\text{CF}} = 6.5, 6.5$ Hz), 122.7, 124.4 (dd,

$J_{\text{CF}} = 8.6, 8.6 \text{ Hz}$), 126.8, 127.4, 127.9, 142.2 (dd, $J_{\text{CF}} = 252, 13 \text{ Hz}$); ^{19}F NMR (470 MHz, CDCl_3): δ 10.4 (s); IR (neat): $\tilde{\nu}$ 1657, 1356, 1242, 1016, 906, 746, 544 cm^{-1} ; HRMS (70 eV, EI): m/z calcd. for $\text{C}_{14}\text{H}_8\text{F}_2$ ($[\text{M}]^+$): 214.0594; found: 214.0595.

4.2.7.2. 5,6-Difluorochrysene (**6b**)

^1H NMR (500 MHz, CDCl_3): δ 7.65–7.76 (m, 4H), 8.01 (d, $J = 8.5 \text{ Hz}$, 2H), 8.22–8.27 (m, 1H), 8.67 (dd, $J = 9.2, 2.3 \text{ Hz}$, 1H), 8.73–8.78 (m, 1H), 9.20 (d, $J = 7.8 \text{ Hz}$, 1H); ^{13}C NMR (126 MHz, CDCl_3): 120.0 (d, $J_{\text{CF}} = 9 \text{ Hz}$), 120.3 (d, $J_{\text{CF}} = 6 \text{ Hz}$), 120.4, 123.1, 123.6 (d, $J_{\text{CF}} = 15 \text{ Hz}$), 126.4 (dd, $J_{\text{CF}} = 3, 3 \text{ Hz}$), 126.7 (d, $J_{\text{CF}} = 2 \text{ Hz}$), 126.9, 127.14, 127.17, 127.3, 127.4, 128.0, 128.5, 128.6 (dd, $J_{\text{CF}} = 5, 5 \text{ Hz}$), 132.7, 144.3 (dd, $J_{\text{CF}} = 215, 14 \text{ Hz}$), 146.3 (dd, $J_{\text{CF}} = 218, 13 \text{ Hz}$); ^{19}F NMR (470 MHz, CDCl_3): δ 12.6 (d, $J = 16 \text{ Hz}$, 1F), 21.6 (d, $J = 16 \text{ Hz}$, 1F); IR (neat): $\tilde{\nu}$ 1647, 1381, 1242, 993, 812, 750, 640 cm^{-1} ; HRMS (70 eV, EI): m/z calcd. for $\text{C}_{18}\text{H}_{10}\text{F}_2$ ($[\text{M}]^+$): 264.0751; found: 264.0744.

4.2.7.3. 5,6-Difluoropicene (**6c**)

60 mg, 63% yield (**6c** + **6c'**, **6c** : **6c'** = 89 : 11), colorless crystals; ^1H NMR (500 MHz, CDCl_3): δ 7.69 (dd, $J = 7.8, 7.8 \text{ Hz}$, 1H), 7.72–7.78 (m, 3H), 8.01 (d, $J = 8.5 \text{ Hz}$, 2H), 8.22–8.27 (m, 1H), 8.78–8.81 (m, 1H), 8.83 (d, $J = 8.3 \text{ Hz}$, 1H), 8.88 (dd, $J = 9.3, 2.0 \text{ Hz}$, 1H), 8.95 (d, $J = 9.3 \text{ Hz}$, 1H), 9.16 (dd, $J = 9.4, 2.9 \text{ Hz}$, 1H); ^{13}C NMR (126 MHz, CDCl_3): 120.5 (dd, $J_{\text{CF}} = 6, 6 \text{ Hz}$), 120.7 (d, $J_{\text{CF}} = 8 \text{ Hz}$), 121.2, 122.2, 123.20, 123.23, 123.23, 123.9 (d, $J_{\text{CF}} = 15 \text{ Hz}$), 124.8, 125.0, 126.8, 127.0 (d, $J_{\text{CF}} = 2 \text{ Hz}$), 127.1, 127.5, 127.8 (d, $J_{\text{CF}} = 3 \text{ Hz}$), 128.3, 129.8, 130.0, 131.9, 132.3, 144.7 (dd, $J_{\text{CF}} = 250, 15 \text{ Hz}$), 146.1 (dd, $J_{\text{CF}} = 253, 13 \text{ Hz}$); ^{19}F NMR (470 MHz, CDCl_3): δ 13.0 (d, $J = 15 \text{ Hz}$, 1F), 22.0 (d, $J = 15 \text{ Hz}$, 1F); IR (neat): $\tilde{\nu}$ 1645, 1250, 1011, 912, 741, 650 cm^{-1} ; HRMS (70 eV, EI): m/z calcd. for $\text{C}_{22}\text{H}_{12}\text{F}_2$ ($[\text{M}]^+$): 314.0907; found: 314.0914; mp: 233–234 °C.

4.2.7.4. 13,14-Difluoropicene (**6e**)

92 mg, 98% yield, yellow crystals; ^1H NMR (500 MHz, CDCl_3): δ 7.69–7.77 (m, 4H), 8.00 (d, $J = 9.3 \text{ Hz}$, 2H), 8.02 (d, $J = 6.5 \text{ Hz}$, 2H), 8.72 (d, $J = 9.3 \text{ Hz}$, 2H), 9.24 (d, $J = 8.5 \text{ Hz}$, 2H); ^{13}C NMR (126 MHz, CDCl_3): δ 121.1, 126.1 (dd, $J_{\text{CF}} = 4, 4 \text{ Hz}$), 127.37, 137.39, 127.62, 127.61 (dd, $J_{\text{CF}} = 30, 5 \text{ Hz}$), 128.1,

128.2, 128.4, 132.6, 148.2 (dd, $J_{CF} = 253$, 17 Hz); ^{19}F NMR (470 MHz, CDCl_3): δ 23.9 (s); IR (neat): $\tilde{\nu}$ 2359, 1433, 1412, 1246, 912, 804, 742 cm^{-1} ; HRMS (70 eV, EI): m/z calcd. for $\text{C}_{22}\text{H}_{12}\text{F}_2$ ($[\text{M}]^+$): 314.0902; found: 314.0907; mp: 243–245 °C.

4.3. Synthesis of other difluorinated PAHs **6f–i**

4.3.1. Preparation of 1,1-difluoro-1-alkenes **1f,g**

Difluoroalkene **1f** was prepared by the Negishi coupling of the corresponding biaryl bromide and 2,2-difluorovinylzinc(II) chloride–TMEDA complex using a PEPPSI-IPr catalyst [27]. Difluoroalkene **1g** was prepared by the Wittig-type difluoromethylideneation of the corresponding aldehyde with $\text{CBr}_2\text{F}_2/\text{P}(\text{NMe}_2)_3$ [6b].

4.3.2. Spectral data of 1,1-difluoro-1-alkenes **1f,g**

4.3.2.1. 1-(2,2-Difluoroethenyl)-3-fluoro-2-(phenanthren-2-yl)benzene (**1f**)

1.15 g, 83% yield, colorless crystals; ^1H NMR (500 MHz, CDCl_3): δ 5.10 (dd, $J = 26.4$, 4.0 Hz, 1H), 7.11 (dd, $J = 8.7$, 8.7 Hz, 1H), 7.38 (ddd, $J = 8.1$, 8.1, 6.0 Hz, 1H), 7.46 (d, $J = 8.0$ Hz, 1H), 7.57 (d, $J = 8.4$ Hz, 1H), 7.63 (dd, $J = 7.4$, 7.4 Hz, 1H), 7.69 (dd, $J = 7.0$, 7.0 Hz, 1H), 7.74–7.83 (m, 3H), 7.92 (d, $J = 7.4$ Hz, 1H), 8.72 (d, $J = 8.0$ Hz, 1H), 8.77 (d, $J = 8.8$ Hz, 1H); ^{13}C NMR (126 MHz, CDCl_3): 80.0 (ddd, $J_{CF} = 32$, 12, 4.0 Hz), 114.2 (d, $J_{CF} = 23$ Hz), 122.7, 122.8, 123.5 (dd, $J_{CF} = 10$, 3 Hz), 126.80, 126.82, 126.9, 127.5, 128.59, 128.65, 128.96, 129.03, 129.8, 130.1, 130.2, 131.1 (ddd, $J_{CF} = 7$, 3, 3 Hz), 131.7, 131.9, 132.2, 156.5 (dd, $J_{CF} = 300$, 289 Hz), 160.1 (d, $J_{CF} = 245$ Hz); ^{19}F NMR (470 MHz, CDCl_3): δ 47.8 (dd, $J_{FH} = 8$, 7 Hz, 1F), 79.0 (dd, $J = 27$ Hz, $J_{FH} = 27$ Hz, 1F), 80.4 (dd, $J = 27$ Hz, $J_{FH} = 4$ Hz, 1F); IR (neat): $\tilde{\nu}$ 1726, 1450, 1261, 904, 889, 812, 741 cm^{-1} ; HRMS (70 eV, EI): m/z calcd. for $\text{C}_{22}\text{H}_{13}\text{F}_3$ ($[\text{M}]^+$): 334.0969; found: 334.0971.

4.3.2.2. 1-(2,2-Difluoroethenyl)-5-fluoro-2-(phenanthren-2-yl)benzene (**1g**)

0.532 g, 77% yield, colorless crystals; ^1H NMR (500 MHz, CDCl_3): δ 5.26 (dd, $J = 25.6$, 4.0 Hz, 1H), 7.06 (ddd, $J = 8.3$, 8.3, 2.6 Hz, 1H), 7.35–7.41 (m, 2H), 7.57 (dd, $J = 8.5$, 1.8 Hz, 1H), 7.63 (dd, $J = 7.5$, 7.5 Hz, 1H), 7.69 (dd, $J = 7.5$, 7.5 Hz, 1H), 7.75 (d, $J = 8.9$ Hz, 1H), 7.77–7.82 (m, 2H), 7.92 (d, $J = 7.8$

Hz, 1H), 8.71 (d, $J = 8.1$ Hz, 1H), 8.73 (d, $J = 8.5$ Hz, 1H); ^{13}C NMR (126 MHz, CDCl_3): 80.4 (ddd, $J_{\text{CF}} = 31, 12, 2$ Hz), 114.2 (d, $J_{\text{CF}} = 21$ Hz), 114.6 (dd, $J_{\text{CF}} = 23, 10$ Hz), 122.7, 122.8, 126.7, 126.79, 126.81, 127.6, 128.1, 128.6, 129.2, 129.4, 129.99, 130.00 (dd, $J_{\text{CF}} = 14, 7$ Hz), 131.85 (d, $J_{\text{CF}} = 14$ Hz), 131.86, 132.1, 136.9, 137.9, 156.5 (dd, $J_{\text{CF}} = 300, 290$ Hz), 162.1 (d, $J_{\text{CF}} = 246$ Hz); ^{19}F NMR (470 MHz, CDCl_3): δ 47.8 (dd, $J_{\text{FH}} = 16, 8$ Hz, 1F), 79.6 (dd, $J = 26$ Hz, $J_{\text{FH}} = 26$ Hz, 1F), 81.0 (dd, $J = 26$ Hz, $J_{\text{FH}} = 4$ Hz, 1F); IR (neat): $\tilde{\nu}$ 1724, 1460, 1242, 991, 924, 814 cm^{-1} ; HRMS (70 eV, EI): m/z calcd. for $\text{C}_{22}\text{H}_{13}\text{F}_3$ ($[\text{M}]^+$): 334.0969; found: 334.0968.

4.3.3. Synthesis of difluorinated PAHs **6f,g**

Cyclization of difluoroalkenes **1f,g** (synthesis of difluorinated PAHs **6f,g**) was performed in a similar manner to those of trifluoroalkenes.

4.3.4. Spectral data of difluorinated PAHs **6f,g**

4.3.4.1. 1,6-Difluoropicene (**6f**)

47% yield (**6f** + **6f'**, **6f** : **6f'** = 89 : 11, ^{19}F NMR based on an internal standard PhCF_3); ^1H NMR (500 MHz, CDCl_3): δ 7.36 (dd, $J = 14.5, 7.3$ Hz, 1H), 7.57 (ddd, $J = 7.8, 7.8, 4.8$ Hz, 1H), 7.66 (d, $J = 15.9$ Hz, 1H), 7.66–7.71 (m, 2H), 7.74 (dd, $J = 7.6, 7.6$ Hz, 1H), 7.97–8.01 (m, 2H), 8.85 (d, $J = 8.5$ Hz, 1H), 9.00 (d, $J = 9.5$ Hz, 1H), 9.18 (dd, $J = 9.5, 3.0$ Hz, 1H), 9.37–9.42 (m, 1H); ^{13}C NMR (126 MHz, CDCl_3): 110.8 (d, $J_{\text{CF}} = 24$ Hz), 112.7 (d, $J_{\text{CF}} = 25$ Hz), 117.4 (d, $J_{\text{CF}} = 8$ Hz), 121.0 (d, $J_{\text{CF}} = 12$ Hz), 123.3, 123.5, 125.3, 125.5, 125.6 (d, $J_{\text{CF}} = 29$ Hz), 126.7, 127.0 (d, $J_{\text{CF}} = 6$ Hz), 127.1, 127.3 (d, $J_{\text{CF}} = 10$ Hz), 127.6, 128.2, 129.4, 129.8, 130.3, 131.8, 134.2 (dd, $J_{\text{CF}} = 11, 4$ Hz), 160.0 (d, $J_{\text{CF}} = 256$ Hz), 161.1 (d, $J_{\text{CF}} = 254$ Hz); ^{19}F NMR (470 MHz, CDCl_3): δ 54.3 (d, $J_{\text{FH}} = 14$ Hz, 1F), 54.5 (d, $J_{\text{FH}} = 16$ Hz, 1F); IR (neat): $\tilde{\nu}$ 1277, 1227, 914, 847, 820, 748, 741 cm^{-1} ; HRMS (70 eV, EI): m/z calcd. for $\text{C}_{22}\text{H}_{12}\text{F}_2$ ($[\text{M}]^+$): 314.0907; found: 314.0907; mp: 187–190 $^\circ\text{C}$.

4.3.4.2. 3,6-Difluoropicene (**6g**)

0.160 g, 57% yield (**6g** + **6g'**, **6g** : **6g'** = 94 : 6), colorless crystals; ^1H NMR (500 MHz, CDCl_3): δ 7.43 (ddd, $J = 8.8, 8.8, 2.6$ Hz, 1H), 7.55 (dd, $J = 9.2, 2.6$ Hz, 1H), 7.62 (d, $J = 16.1$ Hz, 1H), 7.69 (dd, $J =$

7.4, 7.4 Hz, 1H), 7.75 (dd, $J = 6.9, 6.9$ Hz, 1H), 7.98–8.05 (m, 2H), 8.78 (dd, $J = 9.2, 5.3$ Hz, 1H), 8.81–8.88 (m, 2H), 9.03 (d, $J = 9.2$ Hz, 1H), 9.20 (dd, $J = 9.4, 3.4$ Hz, 1H); ^{13}C NMR (126 MHz, CDCl_3): 110.5 (dd, $J_{\text{CF}} = 27, 4$ Hz), 111.2 (dd, $J_{\text{CF}} = 21, 5$ Hz), 115.2 (d, $J_{\text{CF}} = 24$ Hz), 119.8 (d, $J_{\text{CF}} = 11$ Hz), 121.3 (d, $J_{\text{CF}} = 3$ Hz), 123.1, 123.5, 124.5, 125.3 (d, $J_{\text{CF}} = 28$ Hz), 125.8 (d, $J_{\text{CF}} = 9$ Hz), 126.8, 126.9, 127.5 (d, $J_{\text{CF}} = 6$ Hz), 127.9 (d, $J_{\text{CF}} = 3$ Hz), 128.3, 129.3, 130.0, 131.4 (d, $J_{\text{CF}} = 6$ Hz), 131.7, 133.3 (dd, $J_{\text{CF}} = 12, 12$ Hz), 160.5 (d, $J_{\text{CF}} = 255$ Hz), 161.7 (d, $J_{\text{CF}} = 248$ Hz); ^{19}F NMR (470 MHz, CDCl_3): δ 49.5 (dd, $J_{\text{FH}} = 13, 8$ Hz, 1F), 54.5 (d, $J_{\text{FH}} = 16$ Hz, 1F); IR (neat): $\tilde{\nu}$ 1628, 1450, 1263, 912, 872, 806, 746 cm^{-1} ; HRMS (70 eV, EI): m/z calcd. for $\text{C}_{22}\text{H}_{12}\text{F}_2$ ($[\text{M}]^+$): 314.0907; found: 314.0902; mp: 228–230 °C.

4.3.5. Preparation of bis(1,1-difluoroallene)s **7a,b**

p- and *m*-xylenes were converted to the corresponding α,α' -dibromoxylenes using NBS under standard conditions. Benzylic bromides thus obtained were subjected to nucleophilic cyanation using KCN to give α,α' -dicyanoxylenes. Bis(difluoroallene)s **7a,b** were prepared from these dicyanides by the method in our previous papers [14a,b].

4.3.6. Spectral data of bis(1,1-difluoroallene)s **7a,b**

4.3.6.1. 1,4-Bis[1-(3,3-difluoropropa-1,2-dien-1-yl)cyclo-pent-3-en-1-yl]benzene (**7a**)

2.43 g, 35% yield (four steps from α,α' -dicyano-*p*-xylene), a colorless liquid. ^1H NMR (500 MHz, CDCl_3): δ = 2.83 (d, $J = 15.3$ Hz, 4H), 2.88 (d, $J = 15.3$ Hz, 4H), 5.74 (s, 4H), 6.54 (t, $J = 2.4$ Hz, 2H), 7.26 (s, 4H); ^{13}C NMR (126 MHz, CDCl_3): δ = 44.3, 53.3, 126.8, 128.6, 129.5 (t, $J_{\text{CF}} = 6$ Hz), 144.0, 153.0 (t, $J_{\text{CF}} = 263$ Hz), 166.5 (t, $J_{\text{CF}} = 36$ Hz); ^{19}F NMR (470 MHz, CDCl_3): δ = 61.8 (d, $J = 2$ Hz); IR (neat): $\tilde{\nu}$ 2914, 2008, 1435, 1192, 679 cm^{-1} ; HRMS (EI): m/z calcd. for $\text{C}_{22}\text{H}_{18}\text{F}_4$ ($[\text{M}]^+$): 358.1345; found: 358.1359.

4.3.6.2. 1,3-Bis[1-(3,3-difluoropropa-1,2-dien-1-yl)cyclo-pent-3-en-1-yl]benzene (**7b**)

411 mg, 30% yield (four steps from α,α' -dicyano-*m*-xylene), a colorless liquid. ^1H NMR (500 MHz, CDCl_3): δ = 2.86–2.93 (m, 8H), 5.78 (s, 4H), 6.58 (t, $J_{\text{HF}} = 2.1$ Hz, 2H), 7.17–7.20 (m, 3H), 7.32 (dd, $J = 7.7, 7.7$ Hz, 1H); ^{13}C NMR (126 MHz, CDCl_3): δ = 44.3, 53.8, 124.8, 125.2, 128.6, 128.7, 129.7 (t,

$J_{CF} = 6$ Hz), 146.0, 153.0 (t, $J_{CF} = 263$ Hz), 166.6 (t, $J_{CF} = 36$ Hz); ^{19}F NMR (470 MHz, CDCl_3): $\delta = 61.7$ (d, $J_{FH} = 2$ Hz); IR (neat): $\tilde{\nu} = 2918, 2848, 2009, 1435, 1240, 1194, 679$ cm^{-1} ; HRMS (EI): calcd. for $\text{C}_{22}\text{H}_{18}\text{F}_4$ ($[\text{M}]^+$): 358.1345; found: 358.1328.

4.3.7. Synthesis of difluorinated PAHs **6h,i**

Synthesis of difluorinated PAH **6h** [tandem cyclization of bis(1,1-difluoroallene) **7a**] is described as a typical procedure. To a 1,2-dichloroethane solution (5 mL) of bis(difluoroallene) **7a** (36 mg, 0.10 mmol) was added InBr_3 (1 mg, 0.004 mmol) at room temperature. After stirring for 30 min, 2,3-dichloro-5,6-dicyano-*p*-benzoquinone (DDQ, 57 mg, 0.25 mmol) was added in a solid form, and then the resulting solution was refluxed for 1.5 h. After the mixture was cooled to room temperature, the solvent was removed under reduced pressure. The residue was purified by column chromatography on silica gel (hexane) to give 6,7-difluoropicene **6h** as colorless crystals (24 mg, 75% yield).

4.3.8. Spectral data of difluorinated PAHs **6h,i**

4.3.8.1. 6,7-Difluoropicene (**6h**)

^1H NMR (500 MHz, CDCl_3): δ 7.60–7.73 (m, 6H), 7.94–7.97 (m, 2H), 8.76 (d, $J = 7.0$ Hz, 2H), 8.90 (s, 2H); ^{13}C NMR (126 MHz, CDCl_3): 110.6 (dd, $J_{CF} = 12, 12$ Hz), 117.5 (dd, $J_{CF} = 8, 8$ Hz), 122.6, 123.3, 126.0, 127.1, 127.56, 127.61, 131.7 (d, $J_{CF} = 2$ Hz), 132.4 (d, $J = 6$ Hz), 156.0–159.2 (m); ^{19}F NMR (470 MHz, CDCl_3): δ 55.7 (dd, $J = 7, 7$ Hz); IR (neat): $\tilde{\nu}$ 1296, 1213, 914, 876, 748 cm^{-1} ; HRMS (70 eV, EI): m/z calcd. for $\text{C}_{22}\text{H}_{12}\text{F}_2$ ($[\text{M}]^+$): 314.0907; found: 314.0910; mp: 188–190 $^\circ\text{C}$.

4.3.8.2. 6,8-Difluorodibenz[*a,j*]anthracene (**6i**)

86 mg, 76% yield, a pale yellow solid. ^1H NMR (500 MHz, CDCl_3): $\delta = 7.43$ (d, $J_{HF} = 11.5$ Hz, 2H), 7.67 (dd, $J = 7.5, 7.5$ Hz, 2H), 7.73 (dd, $J = 7.5, 7.5$ Hz, 2H), 7.87 (d, $J = 7.7$ Hz, 2H), 8.95 (d, $J = 9.0$ Hz, 2H), 8.96 (s, 1H), 10.02 (s, 1H); ^{13}C NMR (126 MHz, CDCl_3): $\delta = 108.3$ (d, $J_{CF} = 20$ Hz), 114.0 (d, $J_{CF} = 6$ Hz), 116.7, 122.8, 123.1 (d, $J_{CF} = 20$ Hz), 126.1, 127.8 (d, $J_{CF} = 6$ Hz), 128.2 (d, $J_{CF} = 5$ Hz), 128.8, 130.4 (d, $J_{CF} = 5$ Hz), 131.9 (d, $J_{CF} = 10$ Hz), 156.9 (d, $J_{CF} = 253$ Hz); ^{19}F NMR (470 MHz,

CDCl_3): $\delta = 37.2$ (d, $J = 12$ Hz); IR (neat): $\tilde{\nu} = 2940, 1647, 1456, 1074, 839, 721, 634$ cm^{-1} ; HRMS (EI): calcd. for $\text{C}_{22}\text{H}_{12}\text{F}_2$ $[\text{M}]^+$: 314.0907; found: 314.0904.

4.4. Downfield shift of ^{19}F NMR signals of bay fluorines

Preparation and characterization of 9-fluoro-7-methoxy-1-(4-methoxyphenyl)phenanthrene **2f** [6b] and 6-fluorodibenz[*a,h*]anthracene **2g** [6a] were described in our previous papers.

4.5. Polarity, solubility, and mobility of pinpoint-fluorinated picenes

Dipole moments were calculated using the DFT/6-31G* method, implemented in Spartan 14. Solubility measurement of the pinpoint-fluorinated PAHs was described in our previous paper [6a].

To make field effect transistors (FETs), heavily n-doped Si wafers with 200 nm thermal oxide and Au/Ti electrodes were used (the channel width = 500 μm , the channel length = 10 μm). Prior to deposition, the Si wafer was processed as follows: after the successive ultrasonic washing in acetone, in ethanol, and finally in ultrapure water, the Si wafer was exposed to ozone for 10 min, and then exposed to vapour of hexamethyldisilazane (HMDS) for 24 h to make self-assembled monolayer coating on the gate insulator. The wafer was then introduced to a vacuum chamber with the base pressure of 1×10^{-5} Pa. 5-Fluoropicene was thermally evaporated from a Knudsen cell at 180 $^\circ\text{C}$ with the deposition rate of 1 nm/min (total thickness of 5-fluoropicene = 450 nm). The Au/Ti electrodes were quickly wire-bonded to the corresponding terminals of sample holder, and the backside of the Si wafer was bonded by conductive resin to the terminal. The wafer was set to the semiconductor parameter analyser under nitrogen atmosphere (1 atm, 99.99%). The mobility was measured typically by $V_{\text{ds}} = 10$ V with V_{g} scanned between -50 to $+50$ V. The mobility was calculated by fitting the $I_{\text{ds}}-V_{\text{g}}$ plots.

4.6. HOMO and LUMO energy levels of pinpoint-fluorinated picenes

A dichloromethane solution (10 mL) of tetrabutylammonium perchlorate (345 mg) in the cell was degassed with nitrogen for 5 min. The background voltammogram was recorded using Pt as working/counter electrodes and Ag/Ag^+ (AgNO_3 0.01 mol/L) as a reference electrode at 25 $^\circ\text{C}$. To the cell were added a pinpoint-fluorinated PAH (1.5 mg) and ferrocene (0.5 mg), and the sample solution

was degassed with nitrogen (5 min) again. The sample voltammogram was recorded in a similar manner to the background measurement.

Acknowledgments

This research is supported by JSPS KAKENHI Grant Number JP16H04105, JSPS KAKENHI Grant Number JP16H01002, and JSPS KAKENHI Grant Number JP15K05414. Central Glass Co., Ltd. is acknowledged for the generous gifts of $(\text{CF}_3)_2\text{CHOH}$ (HFIP) and Tf_2O . Tosoh-F-Tech, Inc. is acknowledged for the generous gifts of CBr_2F_2 , $\text{CF}_2=\text{CH}_2$, and $\text{CF}_3\text{CH}_2\text{I}$.

References and Notes

- [1] (a) R.G. Harvey, *Polycyclic Aromatic Hydrocarbons: Chemistry and Carcinogenicity*, Cambridge University Press, Cambridge, 1991;
(b) R.G. Harvey, *Polycyclic Aromatic Hydrocarbons*, Wiley-VCH, New York, 1997;
(c) J.C. Fetzer, *Large ($C > 24$) Polycyclic Aromatic Hydrocarbons: Chemistry and Analysis*, Wiley, 2000.
- [2] For reviews, see:
(a) J.E. Anthony, *Angew. Chem. Int. Ed.* 47 (2008) 452–483;
(b) Y. Yamashita, *Sci. Technol. Adv. Mater.* 10 (2009) 024313–024313;
(c) Y. Kubozono, X. He, S. Hamao, K. Teranishi, H. Goto, R. Eguchi, T. Kambe, S. Gohda, Y. Nishihara, *Eur. J. Inorg. Chem.* 2014 (2014) 3806–3819.
- [3] (a) R.E. Banks, B.E. Smart, J.C. Tatlow (Eds.), *Organofluorine Chemistry: Principles and Commercial Applications*, Plenum Press, New York, 1994;
(b) K. Uneyama, *Organofluorine Chemistry*, Blackwell Publishing, Oxford, 2006;
(c) P. Kirsch, *Modern Fluoroorganic Chemistry: Synthesis, Reactivity, Applications*, Wiley-VCH, Weinheim, 2004;
(d) J.-P. Bégué, D. Bonnet-Delpon, *Bioorganic and Medicinal Chemistry of Fluorine*, Wiley, Hoboken, 2008.
- [4] S.D. Sharma, S. Doraiswamy, *Indian J. Pure Appl. Phys.* 21 (1983) 445–452.

- [5] D. Gamota, P. Brazis, K. Kalyanasundaram, J. Zhang (Eds.), *Printed Organic and Molecular Electronics*, Springer, Berlin, 2005.
- [6] (a) K. Fuchibe, T. Morikawa, K. Shigeno, T. Fujita, J. Ichikawa, *Org. Lett.* 17 (2015) 1126–1129;
(b) K. Fuchibe, T. Morikawa, R. Ueda, T. Okauchi, J. Ichikawa, *J. Fluorine Chem.* 179 (2015) 106–115.
- [7] Polyfluorinated PAHs, typically bearing tetrafluorobenzo moieties, have been prepared for developing organic n-type semiconducting materials during the current decade. See:
(a) F. Babudri, G.M. Farinola, F. Naso, R. Ragni, *Chem. Commun.* (2007) 1003–1022;
(b) M.L. Tang, Z. Bao, *Chem. Mater.* 23 (2011) 446–455.
- [8] T. Okazaki, K.K. Laali, *Adv. Org. Synth.* 2 (2006) 353–380.
- [9] For reviews on fluorine introduction into aromatic nuclei, see:
(a) T. Furuya, J.E.M.N. Klein, T. Ritter, *Synthesis* 2010 (2010) 1804–1821;
(b) C. Hollingworth, V. Gouverneur, *Chem. Commun.* 48 (2012) 2929–2942;
(c) M.G. Campbell, T. Ritter, *Chem. Rev.* 115 (2015) 612–633;
(d) P.A. Champagne, J. Desroches, J.-D. Hamel, M. Vandamme, J.-F. Paquin, *Chem. Rev.* 115 (2015) 9073–9174;
See also references cited in ref 6b.
- [10] For the oxidative photocyclization, see:
(a) C.S. Wood, F.B. Mallory, *J. Org. Chem.* 29 (1964) 3373–3377;
(b) R. Lapouyade, N. Hanafi, J.-P. Morand, *Angew. Chem. Int. Ed.* 21 (1982) 766–767;
(c) S. Mirsadeghi, G.K.B. Prasad, N. Whittaker, D.R. Thakker, *J. Org. Chem.* 54 (1989) 3091–3096;
(d) Y. Wang, J. Xu, D. J. Burton, *J. Org. Chem.* 71 (2006) 7780–7784;
(e) H. Li, K.-H. He, J. Liu, B.-Q. Wang, K.-Q. Zhao, P. Hu, Z.-J. Shi, *Chem. Commun.* 48 (2012) 7028–7030;
(f) A.V. Bedekar, A.R. Chaudhary, M.S. Sundar, M. Rajappa, *Tetrahedron Lett.* 54 (2013) 392–396;
(g) Z. Li, R.J. Twieg, *Chem. Eur. J.* 21 (2015) 15534–15539;

(h) T. Matsushima, S. Kobayashi, S. Watanabe, *J. Org. Chem.* 81 (2016) 7799–7806;

(i) S. Banerjee, S. Sinha, P. Pradhan, A. Caruso, D. Liebowitz, D. Parrish, M. Rossi, B. Zajc, *J. Org. Chem.* 81 (2016) 3983–3993;

For the coupling reaction, see:

(j) K. Kamikawa, I. Takemoto, S. Takemoto, H. Matsuzaka, *J. Org. Chem.* 72 (2007) 7406–7408;

(k) H. Tsuji, Y. Ueda, L. Ilies, E. Nakamura, *J. Am Chem. Soc.* 132 (2010) 11854–11855.

[11] (a) Y. Kita, H. Tohma, M. Inagaki, K. Hatanaka, T. Yakura, *Tetrahedron Lett.* 32 (1991) 4321–4324;

(b) J. Ichikawa, S. Miyazaki, M. Fujiwara, T. Minami, *J. Org. Chem.* 60 (1995) 2320–2321;

(c) J.-P. Bégué, D. Bonnet-Delpon, B. Crouse, *Synlett* 2004 (2004) 18–29;

(d) I.A. Shuklov, N.V. Dubrovina, A. Börner, *Synthesis* 2007 (2007) 2925–2943;

(e) T. Dohi, N. Yamaoka, Y. Kita, *Tetrahedron* 66 (2010) 5775–5785.

[12] (a) S.C. Agarwal, G. Lambert, W. Padgett, S. Nesnow, *Carcinogenesis* 12 (1991) 1647–1650;

for the efforts to synthesize difluorinated PAHs, albeit in a non-selective manner, see:

(b) M. Zupan, A. Pollak, *J. Org. Chem.* 40 (1975) 3794–3796;

(c) G.I. Borodkin, I.R. Elanov, V.G. Shubin, *Russ. J. Org. Chem.* 46 (2010) 1317–1322.

[13] (a) J.P. Gillet, R. Sauvetre, J.F. Normant, *Synthesis* 1986 (1986) 538–543;

(b) F. Tellier, R. Sauvêtre, J.F. Normant, Y. Dromzee, Y. Jeannin, *J. Organomet. Chem.* 331 (1987) 281–298;

(c) A. Raghavanpillai, D.J. Burton, *J. Org. Chem.* 69 (2004) 7083–7091.

[14] (a) K. Fuchibe, Y. Mayumi, N. Zhao, S. Watanabe, M. Yokota, J. Ichikawa, *Angew. Chem. Int. Ed.* 52 (2013) 7825–7828;

(b) K. Fuchibe, Y. Mayumi, M. Yokota, H. Aihara, J. Ichikawa, *Bull. Chem. Soc. Jpn.* 87 (2014) 942–949;

(c) K. Fuchibe, H. Imaoka, J. Ichikawa, *Chem. Asian J.* in press, doi: 10.1002/asia.201700870.

[15] Structures of pinpoint-monofluorinated PAHs were recently described by Rossi and Zajc. See ref 10i.

[16] C₆F₆ exhibits a ¹⁹F NMR signal at –162.9 ppm vs. CFCl₃.

- [17] R. Lapouyade, N. Hanafi, J.-P. Morand, *Angew. Chem., Int. Ed. Engl.* 21 (1982) 766–767.
- [18] C.H. Dugan, J.R.V. Wazer, *Compilation of Reported F NMR Chemical Shifts*, Wiley Interscience, New York, 1970.
- [19] B.F. Lutnaes, G. Luthe, U.A.T. Brinkman, J.E. Johansen, J. Krane, *Magn. Reson. Chem.* 43 (2005) 588–594.
- [20] 13-Fluoropicene exhibited p-type semiconducting behavior (mobilities of 6.6×10^{-2} cm²/Vs by vacuum deposition on Au electrodes and 1.3×10^{-4} cm²/Vs by spin casting on Au electrodes). See ref 6a and J. Ichikawa, K. Yamamoto, *Jpn. Kokai Tokkyo Koho JP 2014136700 A 2014072820140728*, 2014.
- [21] Solubilizing substituents such as phenyl or *tert*-butyl groups affect planarity of the molecules because of their steric demand. See:
F.B. Mallory, C.W. Mallory, C.K. Regan, R.J. Aspden, A.B. Ricks, J.M. Racowski, A.I. Nash, A.V. Gibbons, P.J. Carroll, J.M. Bohlen, *J. Org. Chem.* 78 (2013) 2040–2045.
- [22] S. Shinamura, I. Osaka, E. Miyazaki, A. Nakao, M. Yamagishi, J. Takeya, K. Takimiya, *J. Am. Chem. Soc.* 133 (2011) 5024–5035.
- [23] O. L. Griffith, J.E. Anthony, A.G. Jones, D.L. Lichtenberger, *J. Am Chem. Soc.* 132 (2010) 580–586.
- [24] H. O. House, D. S. Crumrine, A.Y. Teranishi, H.D. Olmstead, *J. Am. Chem. Soc.* 95 (1973) 3310–3324.
- [25] T. Fujita, I. Takahashi, M. Hayashi, J. Wang, K. Fuchibe, J. Ichikawa, *Eur. J. Org. Chem.* 2017 (2017) 262–265.
- [26] The Negishi coupling reaction of the bis(trifluorovinyl)zinc complex, prepared from trifluorovinyl lithium (4.0 equiv) and zinc dichloride (2.0 equiv), with triflate **4e** (1.0 equiv) afforded **5e** in 22% yield (¹⁹F NMR, 23 h) without recovery of **4e**.
- [27] T. Fujita, T. Ichitsuka, K. Fuchibe, J. Ichikawa, *Chem. Lett.* 40 (2011) 986–988.